THE IMPACT OF IONS ON RNA APTAMER-AMINOGLYCOSIDE INTERACTIONS

A THESIS SUBMITTED TO
THE GRADUATE SCHOOL OF NATURAL AND APPLIED SCIENCES
OF
MIDDLE EAST TECHNICAL UNIVERSITY

BY

REZZAN FAZLIOĞLU

IN PARTIAL FULFILLMENT OF THE REQUIREMENTS
FOR
THE DEGREE OF MASTER OF SCIENCE
IN
BIOTECHNOLOGY

DECEMBER 2019

Approval of the thesis:

THE IMPACT OF IONS ON RNA APTAMER-AMINOGLYCOSIDE INTERACTIONS

submitted by **REZZAN FAZLIOĞLU** in partial fulfillment of the requirements for the degree of **Master of Science in Biotechnology Department, Middle East Technical University** by,

Prof. Dr. Halil Kalıpçılar
Dean, Graduate School of **Natural and Applied Sciences** _____

Assoc. Prof. Dr. Can Özen
Head of Department, **Biotechnology** _____

Assist. Prof. Dr. Müslüm İlgü
Supervisor, **Biotechnology, METU** _____

Assoc. Prof. Dr. Can Özen
Co-Supervisor, **Biotechnology, METU** _____

Examining Committee Members:

Assoc. Prof. Dr. Salih Özçubukçu
Chemistry, METU _____

Assist. Prof. Dr. Müslüm İlgü
Biotechnology, METU _____

Assoc. Prof. Dr. Can Özen
Biotechnology, METU _____

Assist. Prof. Dr. Leyla Nesrin Kahyaoğlu
Food Engineering, METU _____

Assoc. Prof. Dr. Eda Çelik Akdur
Chemical Engineering, Hacettepe University _____

Date: 13.12.2019

I hereby declare that all information in this document has been obtained and presented in accordance with academic rules and ethical conduct. I also declare that, as required by these rules and conduct, I have fully cited and referenced all material and results that are not original to this work.

Name, Surname: Rezzan Fazlıoğlu

Signature:

ABSTRACT

THE IMPACT OF IONS ON RNA APTAMER-AMINOGLYCOSIDE INTERACTIONS

Fazlıoğlu, Rezzan
Master of Science, Biotechnology
Supervisor: Assist. Prof. Dr. Müslüm İlgü
Co-Supervisor: Assoc. Prof. Dr. Can Özen

December 2019, 57 pages

Aptamers are small nucleic acid or peptide molecules that can bind to specific targets with high affinity. They have been applied for diagnostic, therapeutic and imaging purposes. In order to have the best performance of aptamers, it is worth understanding their structural dynamics. Previous studies have demonstrated that aptamer structures and thus their performances are affected by the surrounding sodium, potassium and magnesium ion concentrations. Based on these findings, we hypothesized that these ions may differently affect the binding affinity of nucleic acid aptamers. In our study, we investigated the effects of varying concentrations of sodium, potassium and magnesium ions on RNA aptamers that bind aminoglycosides. Using Isothermal Titration Calorimetry (ITC) and UV spectrophotometry, four neomycin-B binding RNA aptamers were tested in buffer solutions with different ionic contents. Our findings showed that the presence of magnesium leads to a significant change in both binding mode and affinity; whereas, potassium and sodium only affect the binding affinity of the aptamers. Depending on these results, we performed fluorescence assays with fluorophore-modified aptamers and the same buffers as used before. The change in the fluorescence signal between bound and unbound aptamers verified specific ligand binding and indicated that the concentrations and composition of these

ions alter the three-dimensional structure and consequently affect the binding characteristics of aptamers. The main reason for the observed variation in aptamer performance seems to be the result of aptamers adapting to a predominant structure under a specific buffer condition. Therefore, components of the buffer systems that the aptamers are selected and optimized need to be carefully considered by researchers, because in the light of our results, the binding may get affected once the buffer system is modified by end-users.

Keywords: RNA Aptamers, Metal Ions, Aminoglycosides, Isothermal Titration Calorimetry, UV Spectroscopy

ÖZ

RNA YAPILI APTAMERLERİN AMİNOGLİKOZİTLERLE ETKİLEŞİMİNDE METAL İYONLARININ ETKİSİ

Fazlıoğlu, Rezzan
Yüksek Lisans, Biyoteknoloji
Tez Danışmanı: Dr. Öğr. Üyesi Müslüm İlgü
Ortak Tez Danışmanı: Doç. Dr. Can Özen

Aralık 2019, 57 sayfa

Aptamerler, nükleik asit veya peptit yapıda olabilen ve spesifik hedeflere yüksek afiniteyle bağlanabilen küçük moleküllerdir. Tanı, tedavi ve görüntüleme amaçlı kullanılmışlardır. Aptamerlerden en iyi performansı alabilmek için, onların yapısal dinamiklerini anlamakta fayda vardır. Önceki çalışmalar, aptamer yapılarının ve böylece performanslarının, ortamdaki sodyum, potasyum ve magnezyum iyon konsantrasyonlarından etkilendiğini göstermiştir. Bu bulgulara dayanarak, hipotezimiz bu iyonların, nükleik asit yapılı aptamerlerin bağlanma afinitelerini farklı şekillerde etkileyebileceğidir. Bu çalışmada, farklı konsantrasyonlarda sodyum, potasyum ve magnezyum iyonlarının aminoglikozitlere bağlanan RNA aptamerleri üzerine etkilerini inceledik. İzotermal Titrasyon Mikrokalorimetre (İTK) ve UV Spektrofotometre kullanılarak, neomisin-B antibiyotiğine bağlanan dört RNA aptameri, farklı iyonik içerikte tampon çözeltiler ile test edilmiştir. Elde ettiğimiz sonuçlara göre, magnezyum varlığı aptamerlerin bağlanma modu ile birlikte afinitelerinde de büyük değişikliğe yol açarken; sodyum ve potasyum sadece bağlanma afinitelerini etkilemiştir. Bu sonuçlardan yola çıkarak, florofor-bağlı aptamerler ve önceki tampon çözeltileri kullanarak floresans deneyleri gerçekleştirdik. Bağlanan ve bağlanmayan aptamerlerin floresans sinyallerindeki

değişiklik, bağlanmanın hedefe spesifik gerçekleştiğini doğrulamış ve bu iyonların konsantrasyon ve kompozisyonlarının aptamerlerin üç-boyutlu yapılarını ve buna bağlı olarak bağlanma karakteristiklerini değiştirdiğini göstermiştir. Aptamer performanslarında görülen bu farklılığın temel sebebi, aptamerlerin belirli bir tampon çözelti içinde baskın bir yapıya sahip olmalarından kaynaklanır. Bu nedenle, aptamerlerin seçildiği ve optimize edildiği tampon çözelti sisteminin içeriği araştırmacılar tarafından dikkate alınmalıdır, çünkü bu sonuçların ışığında, son kullanıcının tampon çözeltide yapacağı herhangi bir değişiklik bağlanmayı etkileyebilir.

Anahtar Kelimeler: RNA Aptamerleri, Metal İyonları, Aminoglikozitler, İzotermal Titrasyon Mikrokalorimetresi, UV Spektroskopisi

To my amazing mother…

ACKNOWLEDGEMENTS

I am deeply grateful to my supervisor Asst. Prof. Dr. Müslüm İlgü, for all the time and effort he spent teaching and guiding me. I consider myself very lucky to have the opportunity to work with someone who has such a neverending love and enthusiasm for science, which encouraged me every day. I cannot thank him enough for his endless support, valuable guidance and patience.

I owe a special thanks to my co-supervisor Assoc. Prof. Dr. Can Özen, who helped me with everything I needed in any way he could throughout my studies. His recommendations, contributions, useful criticisms and encouragement are greatly appreciated.

I would like to thank the examining committee members for their participations, helpful comments and feedback.

My deepest gratitude forever belongs to my awesome mom, my precious sister and my dear brother. Thanks for always supporting me in whatever I choose to do with my life. Thanks for always believing in me and giving me your endless love. Most importantly, thank you for always expecting more from me and setting higher goals, but then always going above and beyond to help me achieve them. In other words, thank you for being the best family in the world.

I would like to thank my dear friend Funda Can for always being there when I needed a friendly support and for not leaving me alone in this adventure.

I would like to thank my team members at Ilgu Lab for their friendships and all the support and help they gave me. I am grateful for having the opportunity to learn and grow with them.

I am thankful to Batuhan Akçabozan for his involvement and help with the project. His contributions during the experiments and the data analysis are much appreciated.

This work was supported by the Scientific and Technological Research Council of Turkey (TÜBİTAK) 2232-International Fellowship for Outstanding Researchers Programme, Project No: 118c016.

A part of this project was supported by AdımODTÜ as an Undergraduate Research Project.

TABLE OF CONTENTS

ABSTRACT v

ÖZ vii

ACKNOWLEDGEMENTS x

TABLE OF CONTENTS xii

LIST OF TABLES xiv

LIST OF FIGURES xv

LIST OF ABBREVIATIONS xvi

CHAPTERS 1

1. INTRODUCTION 1

1.1. Nucleic Acids 1

1.1.1. Chemical Structure of Nucleic Acids 3

1.1.2. RNA Folding 6

1.2. Nucleic Acid-Metal Ion Interactions 7

1.2.1. Metal Ion Interactions with RNA 8

1.3. Aptamers 10

1.3.1. Systematic Evolution of Ligands by Exponential Enrichment (SELEX) 11

1.3.2. Aptamer Modifications 14

1.3.3. Structure-Function Relation 15

1.3.4. Riboswitches and Ion Dependency 17

1.4. Aminoglycosides as Aptamer Targets 18

1.4.1. Aminoglycoside Detection with Aptamers 20

2. MATERIALS AND METHODS 25

2.1. Materials 25
2.1.1. Aptamers 25
2.1.2. Antibiotic Targets 27
2.2. Methods 27
2.2.1. ITC Experiments 27
2.2.2. Fluorescence Spectroscopy 31
3. Results and discussion 35
3.1. ITC Results 35
3.1.1. Fluorescence Spectroscopy Results 44
4. CONCLUSION 47
REFERENCES 49
APPENDICES 57
A. ITC Parameters 57

LIST OF TABLES

TABLES

Table 1.1 Comparison of Aptamers and Antibodies 11
Table 1.2 Aptasensors for Aminoglycoside Detection 22
Table 1.3 Aptasensors for Aminoglycoside Detection, Continued 23
Table 2.1 Aptamers used in ITC Experiments 25
Table 2.2 Aptamers used in fluorescence assays 26
Table 2.3 Buffer systems used in experiments 27
Table 2.4 Sample preparation of aptamer solutions for ITC experiments 29
Table 2.5 Sample preparation of titrant (ligand) solutions for ITC experiments 29
Table 2.6 Sample preparation for fluorescence assays 32
Table 3.1 K_d values of aptamer-ligand binding in each buffer system 42
Table 3.2 ΔS values of aptamer-ligand binding in each buffer system 43
Table 3.3 ΔG values of aptamer-ligand binding in each buffer system 43

LIST OF FIGURES

FIGURES

Figure 1.1 Nucleotide Bases and Sugar Structures 4
Figure 1.2 Metal Ion Driven RNA Folding....6
Figure 1.3 Schematic Illustration of a SELEX Procedure 12
Figure 1.4 Structures of Aminoglycosides....19
Figure 2.1 Secondary structures of aptamers used in ITC experiments....26
Figure 2.2 Secondary structures of 6-FAM modified aptamers....26
Figure 2.3 Main parts of an ITC system 28
Figure 2.4 96-Well plate design for aptamer and increasing ligand concentrations..33
Figure 3.1 Binding curves for 31NEO3A-Neomycin B binding in buffers A and B.35
Figure 3.2 Binding curves for 31NEO3A-Neomycin B binding in buffers C and D.36
Figure 3.3 Binding curves for 24m5NEO2A-Neomycin B binding in buffers A and B 37
Figure 3.4 Binding curves for 24m5NEO2A-Neomycin B binding in buffers C and D 38
Figure 3.5 Binding curves for 30NEO4A-Neomycin B binding in buffers A and B.39
Figure 3.6 Binding curves for 30NEO4A-Neomycin B binding in buffers C and D.40
Figure 3.7 Binding curves for 27m2NEO5A-Neomycin B binding in buffers A and B 41
Figure 3.8 Binding curves for 27m2NEO5A-Neomycin B binding in buffers C and D 42
Figure 3.9 Fluorescence measurements obtained from (a) 23m17NEO1A and (b) 25m10NEO2A....44

LIST OF ABBREVIATIONS

ABBREVIATIONS	
DNA	deoxyribonucleic acid
RNA	ribonucleic acid
SELEX	Systematic Evolution of Ligands by Exponential Enrichment
PCR	Polymerase Chain Reaction
RT-PCR	Reverse Transcription Polymerase Chain Reaction
SPR	Surface Plasmon Resonance
ITC	Isothermal Titration Calorimetry
AFM	Atomic Force Microscope
TPP	Thiamine pyrophosphate
NMR	Nuclear Magnetic Resonance
nM	nanomolar
μM	micromolar
mM	millimolar
μL	microliter
mL	milliliter
K_d	dissociation constant
ddH_2O	distilled water

CHAPTER 1

INTRODUCTION

1.1. Nucleic Acids

In the year 1868, a Swiss scientist named Friedrich Miescher was studying the chemical composition of leukocytes and his studies eventually led to the discovery of DNA. He discovered a novel molecule which is resistant to proteases, contains large amounts of phosphorus and lacks sulphur. He figured that this molecule is not a protein or lipid and named it "nuclein" (Dahm, 2008). After this landmark discovery, in the early twentieth century, subsequent studies rapidly expanded the knowledge about this molecule, which is now called deoxyribonucleic acid, DNA. In 1944, Oswald Avery, Colin MacLeod and Maclyn McCarty claimed that DNA was the active carrier of genetic information and not proteins (Avery, Macleod, & Mc Carty, 1944). This theory was later confirmed in 1952 by Alfred Hershey and Martha Chase as a result of their discoveries concerning the mechanism of replication and the genetics of viruses. They observed that bacteria are infected with T2 bacteriophage viral genome but not proteins, and later on, the new viruses produced from the infected bacteria carried only viral DNA (Hershey & Chase, 1952). A year after this discovery, by extending the work of Rosalind Franklin and Maurice Wilkins, the structure of the DNA was confirmed to be a right-handed double helix using X-Ray crystallography (Watson & Crick, 1953). Thanks to all these studies and many more, today we know that DNA is the storage of all the genetic information, and the expression of the genomic material is needed to maintain the biological functions of all living organisms. The flow of genetic information from DNA into RNA and the synthesis of proteins are collectively termed the "central dogma". Francis Crick's version of the central dogma explains the flow of information from the DNA is transcribed into RNA, and then it's translated into proteins (Dahm, 2010).

In the second half of twentieth century, extensive studies on DNA are carried on, and the understanding of how the genetic information is processed in living organisms became more clear. In 1990, the prominent Human Genome Project was initiated. The project aimed to decipher the human genome by drawing a map of the sequences of all the genes in the human genome. Researchers successfully sequenced all 3.2 billion base pairs in less time than initially expected (Chial, 2008). The project was, in fact, a huge success in identifying the genes encoded in the human genome, but it also revealed that the human genome is much more complex, and still a lot of mysteries to be solved. Upon completion of the Human Genome Project in 2003, several follow-up studies were conducted. One of these studies was the Encyclopedia of DNA Elements (ENCODE) project, that aimed to identify all the functional components of the genome (Rosenbloom et al., 2012). The motivation was to determine the role of the remaining components of the genome, once improperly referred to as "junk DNA".

Recent studies have shown that non-coding DNAs have roles in the regulation of transcription and translation; some of them are even transcribed into functional non-coding RNAs such as tRNA, rRNA, regulatory RNAs and long non-coding RNAs (lncRNAs) (Goff & Rinn, 2015). LncRNA used to be considered "transcriptional noise" because they were believed not to code for any proteins (J. Zhang et al., 2019). Surprisingly, extensive studies with lncRNAs identified that they have many vital roles in cellular functions including regulation of gene expression by sequestering miRNAs and transcriptional factors (Azlan, Obeidat, Yunus, & Azzam, 2019) and thus they were associated with embryonic development, some types of cancers, Hepatitis C and other diseases (Nam & Bartel, 2012).

RNA used to be recognized only as a passive carrier of genetic information through central dogma. However, the number of biological functions attributed to folded RNA molecules is still increasing with new studies. RNA has crucial roles in various pathways of cellular metabolism, such as protein synthesis and transportation, alternative RNA splicing, and regulation of translation. Many RNA types have been described over the past years, some called ribozymes having catalytic activities in

biochemical reactions just like enzymes. Some RNAs have important roles in the regulation of gene expression. Other types of functional RNAs include; small nuclear RNAs (snRNAs), needed for intron splicing in the nucleus; the signal recognition particle (SRP), helping protein transportation through membranes; microRNAs (miRNA) small regulatory RNAs involved in gene expression and the ribozymes catalyzing reactions on both RNA and DNA (such as group I introns) (Clancy, 2008). Another important role of RNA in gene regulation is mediated by riboswitches in both prokaryotes and eukaryotes. Riboswitches are RNA sensors that directly affect gene expression upon metabolite binding due to their ability to switch between conformations (Edwards & Batey, 2010). In all of these cases, metal ions play an essential role in providing structural stability, enabling catalytic functions and regulation. By the multifunctional nature of RNA biopolymers, RNA can serve as conformational switches, catalysts for chemical reactions and rigid structural scaffolds (Stampfl, Lempradl, Koehler, & Schroeder, 2007).

1.1.1. Chemical Structure of Nucleic Acids

'Nucleic acid' term refers to polynucleotide chains consisting of nucleotide bases as their monomeric unit. A nucleotide is formed of a heterocyclic nucleobase, either a purine base (A, adenine or G, guanine) or pyrimidine base (C, cytosine; U, uracil or T, thymine), covalently bound with a glycosidic bond to a pentose sugar (a nucleoside), which is attached to a phosphate with a phosphodiester bond at the 5' or 3' end. Nucleotides (NTP, where N may be A: adenosine; G: guanosine; C: cytidine; T: thymidine; or U: uridine) are linked together through phosphate groups by the 5' and 3' hydroxyl groups to form phosphodiester bonds and make up oligonucleotide chains, or attached to additional phosphate groups to form either NDPs with diphosphates, or NTPs with triphosphates. Structures of nucleotides are illustrated in Figure 1.1.

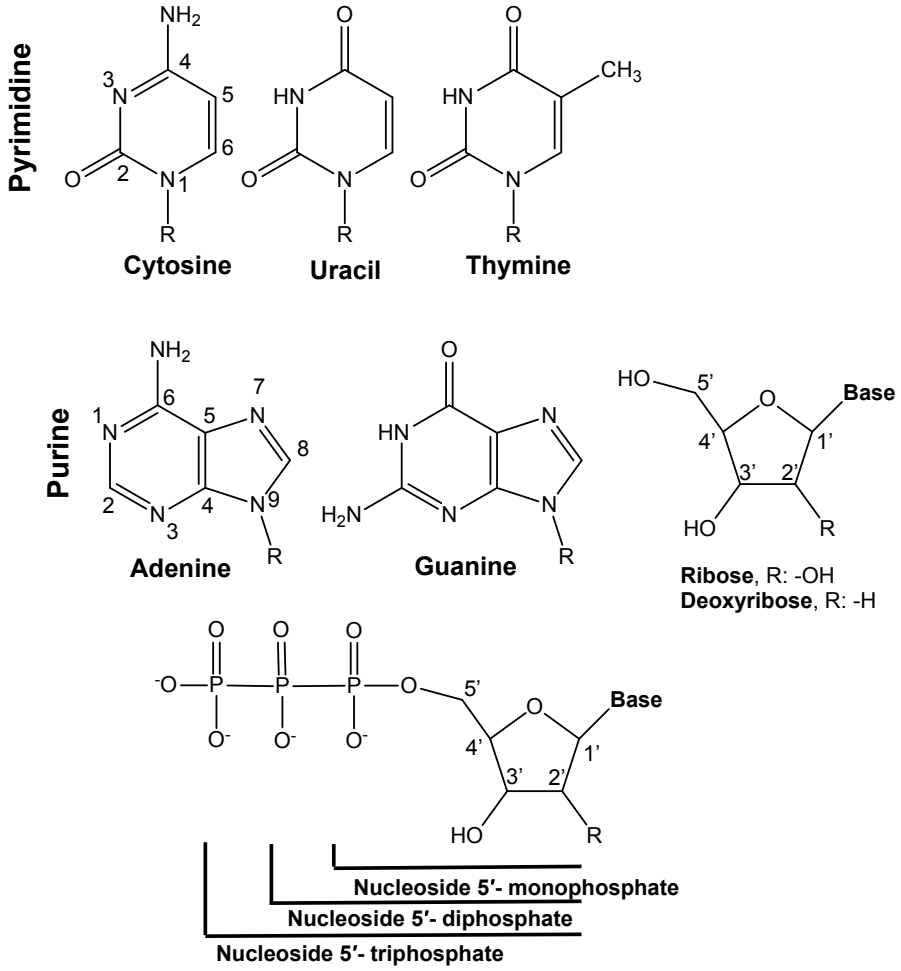

Figure 1.1 Nucleotide Bases and Sugar Structures

The two classes of nucleic acids; ribonucleic acids (RNA) carry a hydroxyl group (-OH) at the 2’ position on the pentose sugar; whereas, deoxyribonucleic acids (DNA) have a hydrogen atom (-H) instead. The heterocyclic bases A, G, C, and T are commonly seen in the DNA, but the T is replaced by U in RNA. These heterocyclic bases are typically planar, and their exocyclic groups lie in the center of the rings, and lonepair electrons are delocalized into the π-systems of the rings. The tautomeric forms of the heterocyclic bases are found in trace concentrations in solution.

Compared to DNA, the 2'-OH group of RNA provides more structural complexity and more options for metal ion binding. Although this 2'-OH group gives RNA a better structural stability under acidic pH conditions, it also makes RNA susceptible to depolymerization due to transesterification caused by polyvalent metal ions at neutral pH.

Water plays an essential role in nucleic acid structure as nucleic acids usually remain highly hydrated in solution. Two H_2O molecules per phosphodiester bond and up to six H_2O per base pair are found in both DNA and RNA. Water interaction with nucleic acids can be classified in two different ways. Firstly, they form hydrogen bonds and create a highly ordered hydration shell around the nucleic acid. This is crucial for intra- and intermolecular interactions between nucleic acid residues and in metal ion-nucleic acid binding, because these sites need to be partially dehydrated to form direct bonds. The second means of water interaction is through a partially ordered water layer weakly bound to the nucleic acid, usually through secondary H-bonds or induced dipole-dipole interactions. These water molecules can be easily replaced with metal ions on the nucleic acid surface. The polarization of water molecules around the nucleic acids can weaken the electrostatic interactions with nucleic acids (Kazakov & Hecht, 2016).

The chemical composition of nucleic acids provides a wide variety of metal-binding sites to form ionic, coordinative (donor-acceptor), hydrogen (-H), and covalent bonds. Specific and nonspecific interactions with metal ions are known to be essential for both RNA folding and stabilization (Lipfert, Doniach, Das, & Herschlag, 2014). To perform all the biological functions, RNA molecules are folded into unique tertiary structures that are highly complex, compact and stable. Even small RNAs are relatively structured chains, which target terminal regions of mRNA for regulating gene expression. A number of RNA structural motifs require certain ions to stabilize the RNA chain. Many ribozymes and riboswitches depend on metal ions as cofactors to form functional configurations (Serganov & Patel, 2012).

1.1.2. RNA Folding

RNA molecules gain their tertiary structures through a two-step process. The first step of RNA folding is the formation of RNA secondary structure, which contains double-stranded regions through complementary base pairing and structural motifs including stem-loops, pseudoknots, internal bulges, hairpins, kissing loops, G-quadruplexes, three-way junction etc. Because of the fact that nucleic acids are highly negatively charged, the RNA molecules depend on cations and molecules to shield the negative charges, so to reduce the repulsion of polyanionic chains. In turn, this shielding promotes folding and helps the RNA adopt a stable secondary structure. Therefore, this process is mediated by monovalent and divalent cations, cationic polyamines, and some basic proteins. Figure 1.2 shows a simplified version of RNA folding pathway and the predominant metal ions involved at each step.

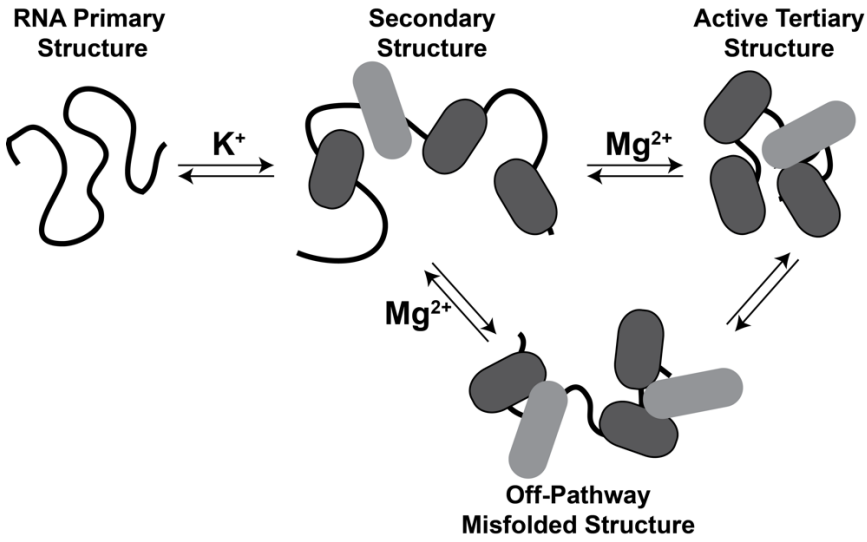

Figure 1.2 Metal Ion Driven RNA Folding

The second stage of RNA folding is the formation of a unique tertiary structure built to perform a specific biological activity. It is formed by intramolecular interactions between bases (base stacking), between sugars (sugar packing) and phosphate backbone. The formation of tertiary structure of RNA is particularly dependent on its sequence, type of metal ions (divalent cations Mg^{2+} and Ca^{2+}; monovalent cations Na^{+} and K^{+}) and RNA's binding partners (RNA binding proteins) (Pyle, 2002).

1.2. Nucleic Acid-Metal Ion Interactions

Metal ions are proven to be essential to maintain structural stability and ensure functionality of the nucleic acids in general (Pyle, 2002). Because nucleic acids are often in contact with metal ions, they are under the influence of the electrostatic interactions. As a result, the thermodynamic stability of their secondary and tertiary structures as well as the kinetic mechanism of RNA folding are affected. (Woodson, 2005).

Close to a hundred metal ions can be found in nature but most of them are not functionally required in biological organisms and some of them are even toxic. Cellular functions like catalysis depend on specific metal ions as cofactors for such reactions (P. Y. Watson & Fedor, 2011). Magnesium (Mg^{2+}) and potassium (K^{+}) are the most frequent ions found in intracellular fluids, whereas the others can be found only in trace amounts and unlikely to interact with nucleic acids. Sodium (Na^{+}) is the most abundant monovalent cation in extracellular fluids, so it's rarely in contact with intracellular nucleic acids (Xi, Wang, Xiong, Zhang, & Tan, 2018). However, it is usually used in the buffer systems to perform binding assays, nuclear magnetic resonance (NMR) spectroscopy (Barnwal, Yang, & Varani, 2017) or X-Ray crystallographic studies (Westhof, 2015) with nucleic acids.

Na^{+} and K^{+} are the two monovalent cations used during structural analyses of nucleic acids. Numerous studies demonstrated that K^{+} is essential for RNA functions. For example, studies report that ribosomal activity is strongly dependent on the presence

of K^+ or ammonium (NH^{4+}) cations but is inhibited by Na^+ (Rozov et al., 2019). Mammalian ribosomes go through a significant unfolding and lose their functions in the absence of K^+ (Näslund & Hultin, 1971). However, several studies indicated that some RNA structural motifs specifically require Na^+ ions for structural stabilization. The stability of hairpin motifs and some ribozymes have been shown to decrease when Na^+ ions were substituted by K^+ ions in the buffer system (Johnson-Buck, McDowell, & Walter, 2011).

Mechanistically, monovalent cations contribute to charge neutralization and help bring the polynucleotide chains together. However, they are usually required in a lot higher concentrations than divalent cations to stabilize the RNA structures. In the absence of divalent cations, they are unable to lead to the active folding of large RNA chains. For example, Na^+ and K^+ cations are needed for the activation of ribozymes, but they don't seem to be directly involved in catalysis (Johnson-Buck et al., 2011). In terms of divalent cations, Mg^{2+} is intracellularly the most abundant and mainly involved in RNA structural stability and functionality. Mg^{2+} has a smaller ionic radius than K^+ and Na^+, and it is the preferred divalent cation for charge neutralization over monovalent ions because of its higher charge density and lower entropic cost for localization (Auffinger, Grover, & Westhof, 2011).

1.2.1. Metal Ion Interactions with RNA

Metal ion binding to RNA usually occurs in two different means; either through diffuse or site-specific binding (ion chelation). "Diffuse ions" are mostly hydrated in a solution and they are attracted to the electrostatic field of RNA. Diffuse binding provides charge shielding and reduces the electrostatic repulsion between RNA backbone. Such shielding can be implemented by a number of mono- or divalent cations that is necessary for RNA to acquire both secondary and tertiary structures (Pyle, 2002). The concentration of diffuse ions in proximity of an RNA molecule is determined by the magnitude of electrostatic potential there. (Draper, 2004). Divalent

Mg^{2+} ions are also shown to diffuse around nucleic acids. So, both monovalent and divalent cations contribute to diffuse ion atmosphere and help stabilization RNA tertiary structure. Although few RNAs can fold into stable tertiary structures with only monovalent ions present, diffuse Mg^{2+} ions are proven to have a significant impact on stabilizing nucleic acids by directly interacting with phosphate backbone (Pyle, 2002). The water ligands of metal ions can interact with RNA bases and backbone substituents on the folded RNA's inner or outer spheres. Outer sphere interactions usually don't have a direct effect on RNA functions, but they are needed to maintain specific motifs. Interactions of metal ions with RNA inner sphere are usually needed for catalytic function (Batey, Rambo, Lucast, Rha, & Doudna, 2000).

The second mechanism of ion interaction is ion chelation. "Chelated ions" can interact with specific sites on the RNA structure directly and they are held in that location by electrostatic forces. K^+ and Mg^{2+} are the cations that mostly interact with other atoms and molecules through electrostatic forces because they both have a closed shell electronic structure. Ion chelation can lead to the displacement of some of the water molecules around diffuse ions on the RNA surface and this has a great energetic cost due to repulsion of these diffuse ions. In order to form direct bonds with RNA, metal ions have to be partially dehydrated. Although, dehydration of Mg^{2+} ions is energetically very expensive, it is required to bring neighboring phosphate groups in close proximity (Draper, 2004). For instance, Mg^{2+} binding to internal loop motifs results in bringing the neighboring chains into an unusual proximity (Correll, Freeborn, Moore, & Steitz, 1997) or dehydrated K+ ion binding to the A-platform motif. The latter interaction inhibits RNA function until the potassium is replaced by thallium (Tl^+) (Basu et al., 1998). On folded RNA molecules, metal ions usually bind to deep and narrow major groove as demonstrated by NMR and X-Ray crystallography (Ferré-D'Amaré & Doudna, 2000). Studies on electrostatic surface potential on RNAs showed that the major groove has a high negative potential, thus, it attracts many ions (Chin, Sharp, Honig, & Pyle, 1999). One of the most common binding sites on the major groove is the tandem G-U wobble base pairs which have a

high negative charge, so it is a preferred binding site for metal ions and coordinated water molecules (Cate & Doudna, 1996).

1.3. Aptamers

Aptamers are single-stranded deoxyribonucleic acid (DNA) or ribonucleic acid (RNA) oligomers or small peptides that bind to their specific targets with high affinity and selectivity. The term "aptamer" is coined from the Latin word *aptus*, which means fit, and the Greek *meros*, meaning part or region. Their potential ligands include proteins and peptides, macromolecules like carbohydrates and lipids, complex molecular suprastructures like viruses and other microorganisms or even whole cells (Dunn, Jimenez, & Chaput, 2017). Aptamers bind to their ligands in a structure-specific manner, by folding into their unique and complex three-dimensional conformations naturally. They are obtained by a selection method called Systematic Evolution of Ligands by Exponential Enrichment (SELEX) (Y. Zhang, Lai, & Juhas, 2019). After selection, oligomers fold and obtain tertiary structural motifs such as stems, loops, bulges, hairpins, pseudoknots, triplexes, or quadruplexes. Although aptamers can be functional in their native 3D forms, they are often further modified with various functional groups to enhance stability, for immobilization and cellular intake. As a result of their high selectivity and affinity to a certain ligand, they have been the preferred tool for many biotechnological applications like diagnostic, therapeutic and imaging purposes. They have also been utilized in drug targeting and novel immunotherapy approaches to treat various diseases (Wengerter et al., 2014).

Due to their similar applications, aptamers and antibodies are often compared. Table shows the main comparison points between aptamers and antibodies. The prominent advantage of aptamers over antibodies is their stability. As they are nucleic acid-based molecules, aptamers are more thermally stable than protein-based antibodies, which go under irreversible degradation at high temperatures; whereas, aptamers can be refolded into their tertiary structures and gain functionality, so they can be used

repeatedly. Nucleic acids are usually not recognized by the human immune system, so aptamers have very low immunogenicity and toxicity in the body. Another important advantage is the ease of aptamer production. While the production of monoclonal antibodies is a very laborious and expensive process which sometimes can take months, upon selection, aptamers can easily be obtained in high amounts with great accuracy using solid state synthesis, during which aptamers can be further modified with other functional groups. Antibody production requires an immune response, so they cannot recognize certain nonimmunogenic ligands such as ions and small molecules for which aptamers show a high affinity and selectivity (Song, Lee, & Ban, 2012).

Table 1.1 Comparison of Aptamers and Antibodies

Feature	Aptamer	Antibody
Molecular Weight	Small (<30 kDa)	Relatively Large (>75 kDa)
Stability	Refolds to functional tertiary structure after denaturation	Irreversibly denatured at high temperatures
Affinity & Specificity	High	High
Targets	Any molecule or cell	Immunogenic molecules
Minimum Target Size	Small, ~60 Da	~600 Da
Immunogenicity	Very low	High
Production time	Several days to weeks	Several months
Reproducibility	Very low batch variation	Very high batch variation
Cost and Manufacture	Cheap, *in vitro*	Expensive, *in vivo*
Chemical Modifications	Easily modified with functional groups	Difficult to chemically modify
Storage	Stable at room tempetature	Easily denaturated, needs freezing
Shelf Life	Several years (if dried)	~6 months

1.3.1. Systematic Evolution of Ligands by Exponential Enrichment (SELEX)

Aptamers are selected against a specific target from a randomized oligonucleotide library by stimulating evolution *in vitro* under a defined set of conditions. This

selection method is called SELEX and it was first discovered in 1990 by three separate groups; namely Tuerk and Gold (Tuerk & Gold, 1990), Ellington and Szostak (Ellington & Szostak, 1990) and Robertson and Joyce (Robertson & Joyce, 1990). SELEX includes a number of selection rounds (5 to 20 rounds); at each round, a random oligonucleotide pool is incubated with the target molecule and the best binding oligonucleotides are isolated for enrichment by PCR amplification (PCR for DNA libraries, RT-PCR for RNA libraries). At the end of these selection rounds, the sequences of the oligonucleotides with the highest affinity toward the target are identified.

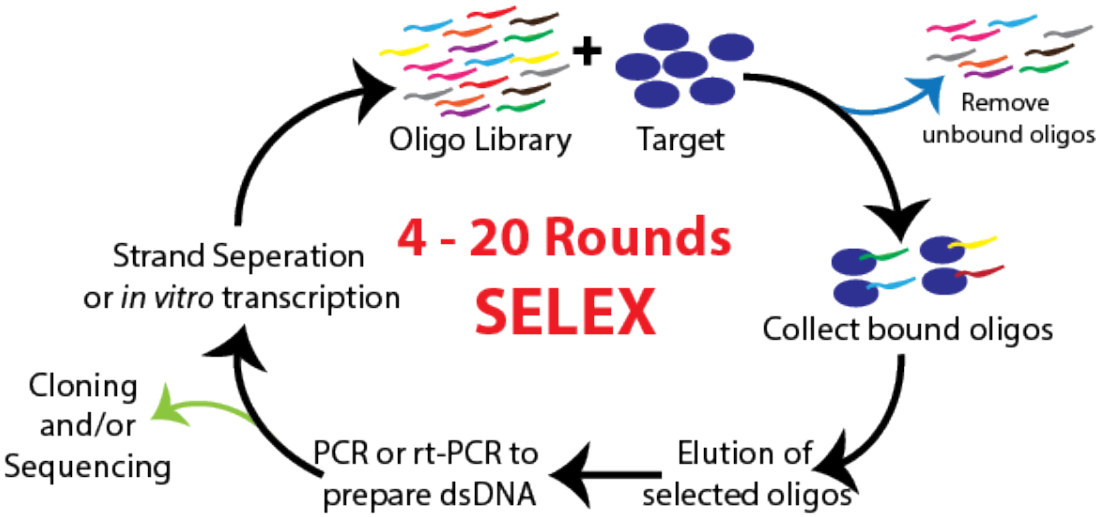

Figure 1.3 Schematic Illustration of a SELEX Procedure

Before a SELEX procedure, a randomized oligonucleotide library is obtained. The initial oligonucleotide libraries usually consist up to 10^{15} unique sequences, which all carry a random region (20-50 nucleotides long) flanked by two fixed primer binding sites for PCR amplification. A conventional SELEX experiment is usually carried in four steps: 1. Incubation of the oligonucleotide pool with the target 2. Partitioning of the binding sequences 3. Amplification of these sequences with PCR 4. Sequencing

the best binding sequences to identify aptamers. Before sequencing the most promising oligonucleotides, first three steps of this procedure are followed for several rounds (5-20 rounds) to amplify the bound sequences. At each round unbound oligos are separated and bound oligos are amplified using PCR for DNA libraries or RT-PCR for RNA libraries. For DNA SELEX, biotin-labeled primers can be used in PCR, and the resulting double-stranded forms are separated using methods such as streptavidin bead capture. For RNA, T7 RNA polymerase promoter containing primers are used in RT-PCR after which RNA libraries are amplified by in vitro transcription. The target molecules are usually immobilized on a matrix to achieve partitioning of the bound oligos. To eliminate the sequences that bind to the matrix in a target-independent manner, a negative selection round is usually included, which is done by passing the oligonucleotide library through the supporting matrix. A similar approach, called counter-selection, utilizes analogs or structurally similar targets to remove the non-specific binding sequences from the mixture. These procedures are applied in most of the modified SELEX methods to ensure that the obtained sequences are selective and specific to the targets. After the final round, the selected oligonucleotides are sequenced to identify the aptamers. Generally, next-generation sequencing is used to obtain sequences of binding oligos from different rounds of selection. Comparative analysis of these sequences shows the recurring motifs involved in recognition of the target. The most promising sequences are amplified and further characterized.

A number of modified SELEX techniques that aim to shorten the time needed for high-affinity aptamer selection or to obtain aptamers specifically designed for certain applications have been developed. For example, Golden et al. suggested photochemical SELEX (photoSELEX) which enables selection of modified aptamers and required fewer number of selection rounds than traditional SELEX methods. The selected aptamers can form photoinduced covalent bonds with their ligands, to make them more specific (Tombelli, Minunni, & Mascini, 2005). A recently developed method that aims to cut down the amount of time and labor required for SELEX is robotic assisted selection procedure. It is a fully automated method that can perform

12 consecutive selection rounds in less than two days and select aptamers against 8 different targets simultaneously, without any manual interruption needed (Breuers, Bryant, Legen, & Mayer, 2019).

1.3.2. Aptamer Modifications

Despite having the advantages of low immunogenicity, easy production, low cost and high thermal stability, aptamers may undergo degradation in cells, and get rapidly extracted from the body through renal filtration. Nucleic acid aptamers are recognized by nucleases, and peptide aptamers are susceptible to protease degradation (Ni et al., 2017). To circumvent these problems, numerous chemical modifications can be implemented for better aptamer stability *in vivo.* Among these chemical modifications, terminal end modifications such as 5' PEGylation and 3' capping with inverted thymidine, and the modifications on the nucleobases, sugar rings or the phosphodiester bonds are the most commonly used ones (Zhuo et al., 2017). Attachment of certain functional groups is also needed for immobilization of aptamers onto solid supports for biosensor development, such as amine ($-NH_2$), thiol (-SH) or carboxyl (-COOH) groups (E. Wang, Wu, Niu, & Cai, 2011).

Although most of the modifications on aptamer structures are usually applied after selection to enhance stability, this can cause a decrease in affinity towards the target because it may prevent the aptamer ligand interaction or alter the structure of the aptamer. Alternative to the traditional selection methods, modified SELEX techniques that utilizes pre-modified nucleotides have been developed in order to obtain inherently stable aptamers with high affinity. Mod-SELEX methods use chemically modified oligonucleotide libraries such as 2'-amino pyrimidines, 2'fluoro pyrimidines or 2'-O-methyl nucleotides (Keefe & Cload, 2008).

To date, hundreds of aptamers against numerous targets have been selected with different SELEX methodologies, and further modified for various applications. Selected aptamers are often used as recognition molecules for biosensor platforms,

which are called “aptasensors”. Aptamers offer many advantages over antibodies, such as their small size, affinity and selectivity, cost effectiveness and most importantly their flexibility and compatibility for novel biosensor designs. Incorporation of aptamers with a diverse range of nanostructures and sensing methodologies has led to the development innovative biosensors, which are highly sensitive and selective; including electrochemical, optical, microcantilever, and acoustic detectors (Mehlhorn, Rahimi, & Joseph, 2018).

Analyzing the binding properties of aptamers is important before using them for research and development purposes. Binding characteristics of aptamers include affinity, kinetics, specificity and buffer sensitivity, which are crucial information for aptamer design and use. In biosensor development, one of the most important aspects of sensing molecules is the affinity towards the target. The high binding affinity of the aptamers is the result of hydrogen bonds, structural compatibility, aromatic ring stacking, hydrophobic and electrostatic interactions and van der Waals forces (Zhuo et al., 2017). Measurement of the binding affinities of aptamers can be done using several biophysical methods; such as Surface Plasmon Resonance (SPR), Isothermal Titration Calorimetry (ITC), Flow Cytometry, Microscale Thermophoresis (MST), Atomic Force Microscope (AFM) etc. ITC is one of the most widely used methods to determine binding affinity of molecular interactions in solution. It is a label-free, quantitative technique to measure the heat release upon aptamer-ligand binding and determine the binding affinity (dissociation constant, K_d), enthalpy changes, stoichiometry and thermodynamic parameters of molecular interactions (Zhuo et al., 2017).

1.3.3. Structure-Function Relation

In order to form stable tertiary structures, RNA requires positive charges to shield the high negative charges on its phosphate backbone and reduce the repulsion between closely packed chains. Thus, metal cations have an essential role in facilitating RNA

folding in order to become biologically functional molecules. An extensive literature is available regarding how the metal ions interact and effect nucleic acid structures and their function. Aptamers are nucleic acids in nature, so they are also affected by the metal ions. Numerous studies show that aptamers may need certain cations to function or get inhibited by the ionic environment. Characterization of aptamers is needed to understand their molecular recognition, because it is important to know their key properties, such as affinity, kinetics, specificity, ion dependence and buffer sensitivity, in order to efficiently use them in diverse applications (Chang, McKeague, Liang, & Smolke, 2014).

Aptamers are nucleic acid molecules with negatively charged structures, so they are highly affected by the positive ions (cations) surrounding them. Their free form in a solution is highly dependent on the electrostatic interactions with specific ions, ionic strength and pH because these factors affect the charge distribution of the aptamers and consequently their ligand interactions. In different ionic conditions, aptamers will follow different folding patterns and thus their binding affinity and selectivity towards their target will be altered. For this reason, the properties of aptamers and their performances in future applications depend on the buffer system used during the SELEX procedure (Ilgu, Fazlioglu, Ozturk, Ozsurekci, & Nilsen-Hamilton, 2019).

Aptamers bind their ligands in a structure-specific manner through their unique tertiary structures, which they naturally fold into with their surrounding ions. Their binding sites are mainly determined by the secondary structural motifs such as stem-loops, hairpin, pseudoknots, internal bulges, kissing loops, three-way junctions and G-quadruplexes. Based on the primary sequences, these motifs can be predicted (Parisien & Major, 2008) and help to determine the binding site on the aptamer's tertiary structure, which accounts for only a short section of the aptamer. To enhance aptamer selectivity and affinity, truncation is an effective way to minimize the sequence and increase the specific contact points and make the aptamer more accessible for ligand binding (Hasegawa, Savory, Abe, & Ikebukuro, 2016).

1.3.4. Riboswitches and Ion Dependency

Riboswitches are non-coding RNA sequences that carry an aptamer domain as sensing element and a downstream expression domain that regulates the transcription and translation. Regulation by riboswitches is possible through conformational changes thanks to their flexible structures upon specific metabolite binding to the aptamer domain. Riboswitches can regulate gene expression through transcription termination, translation inhibition or inducing alternative splicing of mRNA (McCluskey et al., 2019).

A study with thiamine pyrophosphate (TPP) sensing riboswitches showed that interaction with Mg^{2+} is essential for TPP binding and it cannot be substituted by other monovalent or divalent metal ions. The X-ray crystallography studies of the *thiC* TPP riboswitch from *Arabidopsis thaliana* revealed that oxygen atoms are chelated in the pyrophosphate moiety of TPP by only one Mg^{2+} ion when TPP is bound to the RNA. On the other hand, when the *thiM* riboswitch from *Escherichia coli* is bound to TPP, two bridging Mg^{2+} ions chelate oxygen atoms in the pyrophosphate region. In case of this system, the presence of Mg^{2+} ions is strictly needed for binding of TPP to its riboswitches. However, some riboswitches do not depend on Mg^{2+} ions specifically to function. For example, it was shown that the GlmS riboswitch, which is a ribozyme that undergoes self-cleavage when it interacts with glucosamine-6-phosphate (GlcN6P), does not rely on Mg^{2+} ions for this reaction. Here, the system only requires the positive charges for the electrostatic stabilization of the structure, so high concentrations of monovalent cations, other divalent cations or $Co(NH_3)_6^{3+}$ can substitute Mg^{2+} ions. (Noeske, Schwalbe, & Wöhnert, 2007).

In another work, which investigates the effect of Mg^{2+} ions on conformational dynamics and affinity of *B. subtilis lysC* lysine-binding riboswitch, it was shown that sub-millimolar concentrations of Mg^{2+} have a huge impact on aptamer function and affinity by altering the conformation. This study confirmed that cellular

concentrations of Mg^{2+} cations are high enough to affect RNA functions, stabilize their structures, and also play a role in modulation of gene expression (McCluskey et al., 2019).

1.4. Aminoglycosides as Aptamer Targets

Aminoglycosides are a large family of potent antibiotics that target bacterial ribosome and disturb its functionality. They can bind to the ribosomal decoding site (A-site) or to several ribozymes and inhibit their activity. Aminoglycosides have hydrophilic structures, so they need an electron transport system from the host's respiratory system to penetrate the hydrophobic cell membranes of the bacteria. As a result, they are only effective against aerobic bacteria (Germovsek, Barker, & Sharland, 2017; Krause, Serio, Kane, & Connolly, 2016). In the cytosol, they bind to the 16S rRNA decoding region (A-site) on the 30S small subunit of the bacterial ribosome. Upon aminoglycoside binding, the position of the two adenines, A1492 and A1493, which are needed for the codon–anticodon interaction, get shifted; so, the protein synthesis is inhibited (Fourmy, Recht, Blanchard, & Puglisi, 1996; Ramakrishnan, 2002).

Aminoglycosides are highly flexible molecules with multiple positive charges, which facilitate their binding to the negatively charged major grooves of a variety of RNA molecules (Vakulenko & Mobashery, 2003). It was shown that aminoglycoside binding leads to displacement of divalent metal ions required for both RNA and ribozyme functionality. A study revealed structural data for a small RNA representing 16S rRNA decoding region in complex with several aminoglycosides using NMR spectroscopy. They showed that divalent Pb^{2+} ions induce cleavage on various sites on rRNA A-site which are needed for functionality, and upon binding with aminoglycoside neomycin B, Pb^{2+} induced cleavages are inhibited. This data, along with other similar studies, suggest that binding of aminoglycosides to rRNA A-site leads to divalent ion displacement, hence causing dysfunctionality (codon misreading)

(Butcher, Dieckmann, & Feigon, 1997; Mikkelsen, Johansson, Virtanen, & Kirsebom, 2001).

Aminoglycosides contain a highly conserved aminocyclitol ring to which amino sugars are attached by glycosidic linkages. The aminocyclitol ring consists of a 2-deoxystreptamine (2-DOS) and has 1,3-diamino functionality and three or four hydroxyl groups to bind amino sugars. Aminoglycosides are generally divided into three structural subclasses depending on the position of these glycosidic linkages: 4-monosubsituted, 4,5- or 4,6-disubsituted (Kulik, Goral, Jasiński, Dominiak, & Trylska, 2015). Despite the differences in their substitutions, aminoglycosides in each subclass have high structural resemblance. Figure 1.4 illustrates the chemical structures of aminoglycosides.

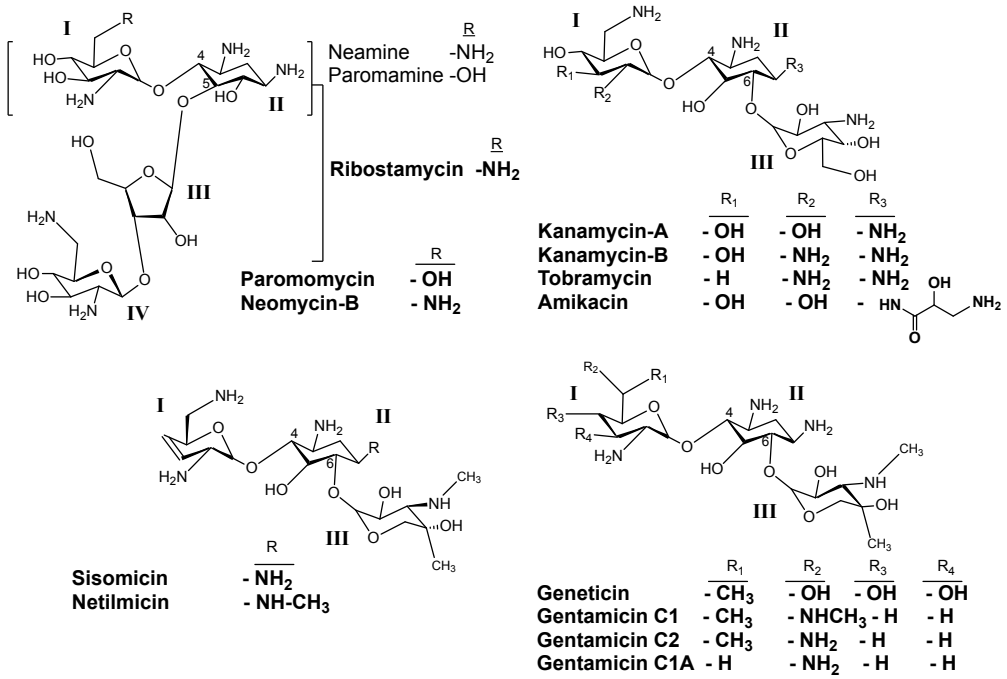

Figure 1.4 Structures of Aminoglycosides

4-monosubstituted aminoglycosides include neamine, paromamine and apramycin, among which apramycin is the only one used pharmaceutically and it carries a bicyclic ring 1. Paromamine and neamine only differ in their R substituent groups and they are not used as drugs alone.

4,5-disubstituted aminoglycosides include ribostamycin, butirosin B, neomycin B, paromomycin and lividomycin A. The antibiotics in this group differ in their substitutions on the third ring. Lividomycin A is the only aminoglycoside in this group that contains five rings.

Kanamycin A, kanamycin B, kanamycin C, tobramycin, sisomicin, netilmicin and amikacin are in a subcategory of 4,6-disubstituted aminoglycosides, and the other subcategory includes gentamicin C1, gentamicin C2, gentamicin C1A and geneticin. The major reason of dividing this group into such subcategories is the presence of an extra R group attached to the 6' position of the first ring as well as the third ring connected to the 2-DOS (Chittapragada, Roberts, & Ham, 2009).

1.4.1. Aminoglycoside Detection with Aptamers

A number of high affinity aptamers have been selected against aminoglycosides such as neomycin B (Wallis, von Ahsen, Schroeder, & Famulok, 1995), tobramycin (Wang & Rando, 1995), lividomycin, kanamycin A (Lato, Boles, & Ellington, 1995) and kanamycin B (Kwon, Chun, Jeong, & Yu, 2001). These selections were done using libraries that have 30 to 74 nucleotide long random regions (Klug & Famulok, 1994). Selections against aminoglycosides resulted in isolation of aptamers that could promiscuously bind to other types of aminoglycosides more or less specifically, due to not applying counterselection procedures. For example, Kwon et al. selected the K8 aptamer originally to bind kanamycin B, but it was shown to have 10-times higher affinity against tobramycin (Kwon et al., 2001). Another aptamer (W13 RNA) was isolated to bind tobramycin, which could recognize neomycin too. Similarly, it is known that most of the lividomycin aptamers can recognize neomycin B and

paromomycin as well (Lato et al., 1995). Based on the outcome of these studies, it is clear that most aminoglycoside-binding aptamers are structurally similar, although they might have different primary sequence and binding patterns. In general, the aminoglycoside-binding RNA aptamers have stem-loop structures and the stems often carry internal bulges or small hairpin loops, resulting in a widened major groove. The loops, essential for binding are quite variable in sequence but seem to show a recurring motif (Lorenz & Schroeder, 2006).

Structural studies of tobramycin and neomycin aptamers revealed similarities in binding patterns; the loops are closed with non-canonical base pairing and the antibiotic is trapped in the major groove (L Jiang et al., 1999; Licong Jiang, Suri, Fiala, & Patel, 1997). Also, neomycin riboswitches selected in yeast shared this structural feature (Weigand et al., 2011).

Since their discovery in the 1940s, aminoglycosides have been the most commonly used antibiotics around the world due to their high efficiency as bactericidal drugs and their low cost. Antibiotics are often misused for humans or in veterinary medicine and in the food industry, for example as growth enhancers in livestock. The unnecessary intake of antibiotics leads to the evolution of antibiotic-resistant bacteria which has recently become a serious problem. This results in current antibiotics losing their effectiveness in treating microbial diseases (Furusawa, Horinouchi, & Maeda, 2018). According to the reports, infections with antibiotic-resistant bacteria account for approximately 33000 deaths each year (Cassini et al., 2018). There have been several successful initiatives to prevent misuse of antibiotics.

In parallel, researchers have successfully developed aptasensors to detect antibiotics in body fluids, remnants in dairy products and food samples in several laboratories today. Selected examples of developed aptasensors for aminoglycoside detection are summarized in Table 1.2.

Table 1.2 Aptasensors for Aminoglycoside Detection

Target	Nucleotide Backbone	Sequence	Dissociation Constant (Kd, nM)	Aptasensor Type/Detection Method	Limit of Detection (LOD, nM)	Reference
Neomycin B	RNA	GGA CUG GGC GAG AAG UUU AGU CC	115 ± 25	Fluorometric	10	(Ling et al., 2016; Wallis et al., 1995)
		GGC CUG GGC GAG AAG UUU AGG CC		Impedimetric Electrochemical	<1000	(De-los-Santos-Álvarez et al., 2007)
		GGC CUG GGC GAG AAG UUU AGG CC	2500 ± 900	Impedimetric Electrochemical	5	(De-los-Santos-Álvarez et al., 2009)
		GGC CUG GGC GAG AAG UUU AGG CC		Electrochemiluminesance	0.017	(Feng et al., 2019)
Kanamycin	DNA	TGG GGG TTG AGG CTA AGC CGA C	78.8	Cantilever Aptasensor	5000	(Bai et al., 2014)
		TGG GGG TTG AGG CTA AGC CGA	78.8	Colorimetric/UV-Vis	25	(Song et al., 2011)
		TGG GGG TTG AGG CTA AGC CGA	78.8	Colorimetric/UV-Vis		(Niu et al., 2014)
		TGG GGG TTG AGG CTA AGC CGA	8.38	Colorimetric Aptasensor	1.49	(Kumar Sharma et al., 2014)
		TGG GGG TTG AGG CTA AGC CGA	78.8	Colorimetric/UV-Vis	0.014	(Zhou et al., 2014)
		TGG GGG TTG AGG CTA AGC CGA	78.8	Colorimetric Aptasensor	4.5	(Y. Xu et al., 2015)
		CGG AAG CGC GCC ACC CCA TCG GCG GGG GCG AAG CTT GCG	92.3 ± 29.1	Colorimetric Aptasensor	3.35	(Ha et al., 2017; Ha et al., 2017)
		TGG GGG TTG AGG CTA AGC CGA		Colorimetric Aptasensor	0.0778	(J. Liu et al., 2018)
		TGG GGG TTG AGG CTA AGC CGA		Liquid Crystal Assay	<1	(Ying Wang et al., 2017)
		AGA TGG GGG TTG AGG CTA AGC CGA		Fluorometric	0.612	(Khabbaz et al., 2015)
		TGG GGG TTG AGG CTA AGC CGA		Fluorometric	1.58	(C. Liu et al., 2015)
		TGG GGG TTG AGG CTA AGC CGA		Electrochemiluminesance	0.35	(Feng et al., 2019)
		GGG ACT TGG TTT AGG TAA TGA GTC CC	650,000	Amperometric Electrochemical/ Square Wave Voltammetry		(Rowe et al., 2011; Wang and Rando, 1995)
	RNA	GGG ACU UGG UUU AGG UAA UGA GUC CC	281,000	Amperometric Electrochemical/ Square Wave Voltammetry		
		GGG ACU UGG UUU AGG UAA UGA GUC CC (fully O-methylated)	450,000	Amperometric Electrochemical/ Square Wave Voltammetry		
Gentamicin	RNA	GGG ACU UGG UUU AGG UAA UGA GUC CC	72,000	Amperometric Electrochemical/ Square Wave Voltammetry		(Rowe et al., 2011; Wang and Rando, 1995)
		GGG ACU UGG UUU AGG UAA UGA GUC CC (fully O-methylated)	80,000	Amperometric Electrochemical/ Square Wave Voltammetry		
	DNA	GGG ACT TGG TTT AGG TAA TGA GTC CC	800,000	Amperometric Electrochemical/ Square Wave Voltammetry		

Table 1.3 Aptasensors for Aminoglycoside Detection, Continued

Target	Nucleotide Backbone	Sequence	Dissociation Constant (Kd, nM)	Aptasensor Type/Detection Method	Limit of Detection (LOD, nM)	Reference
Tobramycin	DNA	TCC GTG TAT AGG TCG GGT CTC TTG CCA ACT GAT TCG TTG AAA AGT ATA GCC CCG CAG GG	260	Surface Plasmon Resonance	500	(Cappi et al., 2015; Spiga et al., 2015)
		TAG GGA ATT CGT CGA CGG ATC CAT GGC ACG TTA TGC GGA GGC GGT ATG ATA GCG CTA CTG CAG GTC GAC GCA TGC GCC G	56.9	Colorimetric Aptasensor	37.9	(Han et al., 2018)
		CGT CGA CGG ATC CAT GGC ACG TTA TGC GGT ATG ATA GCG CAG GTC GAC G	46.8	Colorimetric Aptasensor	37.10	
		CGT CGA CGG ATC CAT GGC ACG TTA TAG GTC GAC G	48.4	Colorimetric Aptasensor	37.11	
		GGG ACT TGG TTT AGG TAA TGA GTC CC		Colorimetric Aptasensor	23.3	(Ma et al., 2018)
	RNA	GGC ACG AGG UUU AGC UAC ACU CGU GCC	400	Impedimetric Electrochemical/ Faradaic Impedance Spectroscopy	400	(González-Fernández et al., 2011; Wang and Rando, 1995)
Streptomycin	DNA	GGG GTC TGG TGT TCT GCT TTG TTC TGT CGG GTC GT	199.1	Colorimetric/UV-Vis	200	(Zhou et al., 2013)
		TGA AGG GTC GAC TCT AGA GGC AGG TGT TCC TCA GG	221.3	Colorimetric/UV-Vis		
		AGC TTG GGT GGG GCC ACG TAG AGG TAT AGC TTG TT	272.0	Colorimetric/UV-Vis		
		TGT GTG TTC GGT GCT GTC GGG TTG TTT CTT GGT TT	340.6	Colorimetric/UV-Vis		
		TAG GGA ATT CGT CGA CGA ATC CGG GGT CTG GTG TTC TGC TTT GTT CGTB TCG GGT CGT CTG CAG GTC GAC GCA TGC GCC G	199.1	Colorimetric Aptasensor	86	(Zhao et al., 2017; Zhou et al., 2013)
		TAG GGA ATT CGT CGA CGG ATC CGG GGT CTG GTG TTC TGC TTT GTT CTG TCG GGT CGT CTG CAG GTC GAC GCA TGC GCC G		Photoelectrochemical Aptasensor	0.033	(X. Xu et al., 2017)
		TAG GGA ATT CGT CGA CGG ATG CGG GGT CTG GTG TTG TGC TTT GTT CTG TCG GGT CGT CTG CAG GTC GAC GCA TGC GCC G		Amperometric Electrochemical/Differential Pulse Voltammetry	11.4	(Danesh et al., 2016)

CHAPTER 2

MATERIALS AND METHODS

2.1. Materials

2.1.1. Aptamers

All aptamers used in this project were purchased as lyophilized from Integrated DNA Technologies (IDT, Coralville, IA). They were then resuspended in sterile MiliQ water (RNase-free) to prepare 1mM stock solutions. Stocks were stored in -20 ºC and kept on ice while sample preparations. All of the aptamers used in this research are single-stranded RNA aptamers. Their sequences are given in Table 2.1 and Table 2.2, and secondary structures with the lowest free energies are illustrated in Figure 2.1 and Figure 2.2 (RNAstructure Web Servers for RNA Secondary Structure Prediction, Matthews Lab, https://rna.urmc.rochester.edu/RNAstructureWeb/).

Table 2.1 Aptamers used in ITC Experiments

Aptamer	**Backbone**	**Size**	**Sequence**
31NEO3A	RNA	31nt	GGC AUA GCU UGU CCU UUA AUG GUC CUA UGU C
24m5NEO2A	RNA	24nt	CAC UGC AGU CCG AAA GGG CCA GUG
30NEO4A	RNA	30nt	CUU UGC GAU GUC CUU UAA UGG UCC GCG AGG
27m2NEO5A	RNA	27nt	GGC UGC UUG UCC UUU A/2AP/U GGU CCA GUC

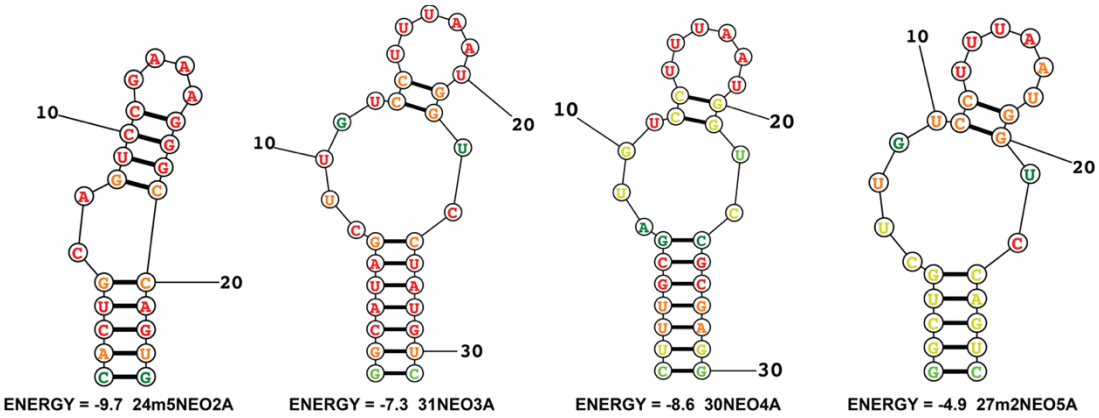

Figure 2.1 Secondary structures of aptamers used in ITC experiments

Table 2.2 Aptamers used in fluorescence assays

Aptamer	**Backbone**	**Size**	**Sequence**
23m17NEO1A	RNA	23nt	GGA CUG GGC GAG /6-FAM/AG UUU AGU CC
25m10NEO2A	RNA	25nt	CAC UGC /6-FAM/GU CCG AAA AGG GCC AGU G

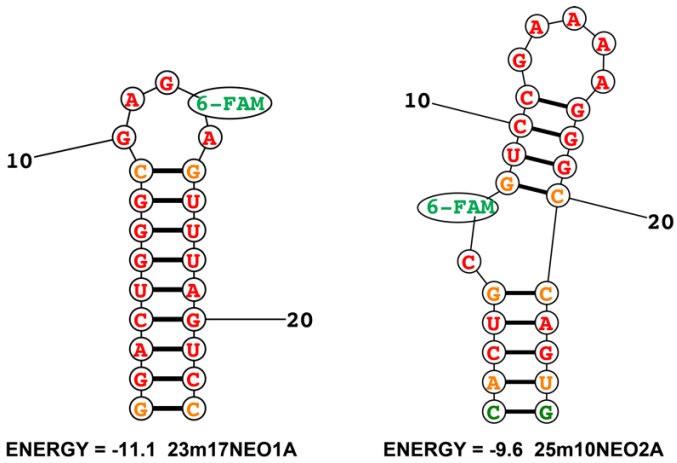

Figure 2.2 Secondary structures of 6-FAM modified aptamers

2.1.2. Antibiotic Targets

Neomycin-B (Sigma; Catalog number: N6910-25G, Lot number: 081K08832), Kanamycin-B (Sigma; Catalog number: B5264-100MG; Lot number: 099K1597) were purchased from Sigma Aldrich and Ampicillin (AppliChem, Catalog number: A6352,0025; Lot number: 6L008514) was purchased from AppliChem BioChemica. Stock solutions of 20 mM were prepared using sterile MiliQ water (RNase-free) and they were stored in -20 ^{o}C until they were used for experiments.

Table 2.3 Buffer systems used in experiments

Buffers	**Ionic Compositions**
A	20 mM Na_2HPO_4, pH 7.4
B	20 mM Na_2HPO_4 + 5 mM $MgCl_2$, pH 7.4
C	20 mM Na_2HPO_4 + 125 mM KCl, pH 7.4
D	20 mM Na_2HPO_4 + 125 mM KCl + 5 mM $MgCl_2$, pH 7.4

2.2. Methods

2.2.1. ITC Experiments

Isothermal Titration Calorimetry (ITC) is a thermoelectric device that measures the temperature difference between the two cells (sample and reference cells) and a second sensor measures the temperature difference between the cells and the jacket. The result is given as the integral of the power required to keep the two cells at a constant temperature over time, which is equal to the change in heat resulting from the process.

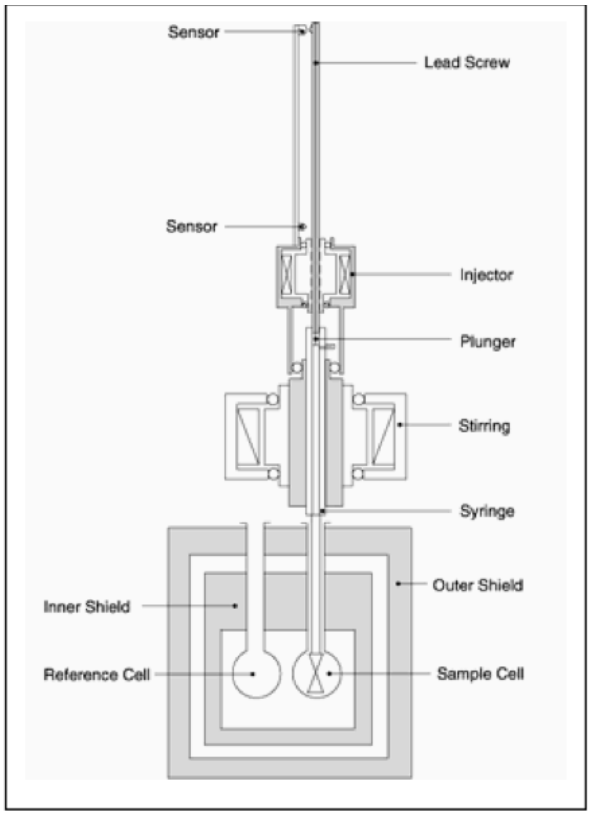

Figure 2.3 Main parts of an ITC system

The change in measured heat release upon ligand binding is directly proportional to binding strength. Ligand is titrated from the syringe in 30 injections into the sample cell containing aptamer solution. Once the aptamer is saturated with ligand, heat signal decreases. Calculated heat release from the injections gives either a hyperbolic or sigmoidal curve, which can be fit to one or two sets of binding site models, from which we can calculate the binding affinity (dissociation constant, K_d), stoichiometry, ΔH (enthalpy), ΔS (entropy) and ΔG (Gibbs free energy) of aptamer-ligand interaction (Duff, Grubbs, & Howell, 2011).

Before an ITC measurement, the equipment is thoroughly washed to avoid contamination or dilution. The sample cell is washed with 30 mL of ddH2O and 10 mL of binding buffer. The syringe is washed with 30mL of ddH_2O and 10 mL of binding buffer as well.

The reference cell is filled with degassed ddH_2O and sealed tightly.

Table 2.4 Sample preparation of aptamer solutions for ITC experiments

	Volume	**Final Concentration**
Aptamer	2.5 μL	2.5 μM
Binding Buffer	200 μL	20 mM (for NaP), 125 mM (for KCl), 5 mM (for $MgCl_2$)
ddH_2O	797.5 μL	
Total	**1 mL**	

Table 2.5 Sample preparation of titrant (ligand) solutions for ITC experiments

	Volume	**Final Concentration**
Neomycin-B	3 μL	60 μM
Binding Buffer	200 μL	20 mM (for NaP), 125 mM (for KCl), 5 mM (for $MgCl_2$)
ddH_2O	797μL	
Total	**1 mL**	

Aptamer solutions were prepared to have a final concentration of 2.5 μM with each buffer system shown in Table 2.4. All the aptamers are single-stranded RNA aptamers,

so, to ensure that they are folded in their correct three-dimensional conformations after unfreezing, a refolding process is required. After aptamer solution is prepared in 1.5 mL Eppendorf tubes, they are placed in 95 ^{o}C heating block for 2 minutes to unfold all the nucleic acid chains, then it is cooled slowly on the bench to room temperature for 90 minutes to allow refolding.

Titrant solutions with neomycin-B ligand were prepared to have a final concentration of 60 μM in the same buffers as the aptamers as shown in Table 2.5. For a typical ITC experiment, the titrant is prepared in about 20-fold higher concentration than the macromolecule. This way proper saturation can be achieved, and the resulting curve would be fit well.

For each ITC experiment, the aptamer and ligand solutions were prepared according to the volumes given in Table 2.4 and Table 2.5. The tubes were carefully vortexed and spun down then the solutions are transferred to 5 mL glass vials. Both samples were degassed using a MicroCal ThermoVac sample degassing thermostat for approximately 5 minutes at 20 ^{o}C. This step is crucial for any ITC run, to avoid any air bubbles in the samples.

The samples were loaded in the MicroCal VP-ITC machine. The aptamer solution was transferred to the sample cell using a long needle Hamilton syringe. The injection syringe was filled with the titrant solution with the help of a plastic disposable syringe. The sample in the syringe was purged and refilled three times automatically using the VPViewer 2000 software.

The parameters for each ITC run are given in the Appendix A.

All the ITC assays were done in at least two repeats. The blank run for each experiment was performed by titrating the ligand samples into the buffer systems with same concentrations of ions.

The analysis of the obtained data was carried out using Origin 7 software. The data from the blank run was subtracted from the aptamer-ligand titration and the released heat values were fit to one or two sets of binding models to obtain the thermodynamic parameters, such as K_d, stoichiometry, ΔH (enthalpy), ΔS (entropy) and ΔG (Gibbs free energy).

2.2.2. Fluorescence Spectroscopy

Aptamers might obtain different conformations in their free and bound states in solution. Fluorophore-labelled aptamers work in signal-on or signal-off modes, depending on the structural change upon ligand binding either exposing or hiding the fluorophore, respectively. The change in fluorescence signal relatively shows the specificity of the aptamer towards the ligand. In these fluorescence assays, the aim is to test the ion-dependency of these aptamer applications. In addition, we may get some information about the effects of different ionic compositions on the conformational change of the same aptamers.

Two aptamers were labelled with 6-FAM (6-Carboxyfluorescein) fluorophore which has an excitation wavelength of 495 nm and an emission wavelength of 517 nm for fluorescence assays. 23m17NEO1A (Ilgu et al., 2014) was tagged at the 13th residue on its pentaloop, and 25m10NEO2A (from the same family as 24m5NEO2A) was tagged at the 7th residue on its internal bulge, as shown in Figure 2.2. Aptamers were prepared in final concentrations of 2.5 μM in the same buffers, as given in Table 2.6. The aptamer samples were placed in the heating block at 95 ^{o}C for 2 minutes to unfold

and slowly cooled on the bench at room temperature for 90 minutes to assure proper refolding.

Table 2.6 Sample preparation for fluorescence assays

	Volume	**Final Concentration**
Aptamer (10 μM in stock)	2.5 μL	2.5 μM
Antibiotic (10x in stock)	10 μL	Varying concentrations, NeoB (0.1 μM-10 μM), KanB (0.5 μM-50 μM), Amp (0.5 μM-50 μM)
Binding Buffer (2x in stock)	48.75 μL	20 mM (for NaP), 125 mM (for KCl), 5 mM (for $MgCl_2$)
ddH_2O	48.75 μL	
Total	**100 μL**	

An aminoglycoside kanamycin and a penicillin type antibiotic ampicillin were used as control groups. Neomycin-B, kanamycin-B and ampicillin antibiotics were prepared in increasing concentrations as given in the Figure 2.4, in the same buffers as aptamers.

96 well Greiner black plates were used for fluorescence assays. Plate design is illustrated in Figure 2.4.

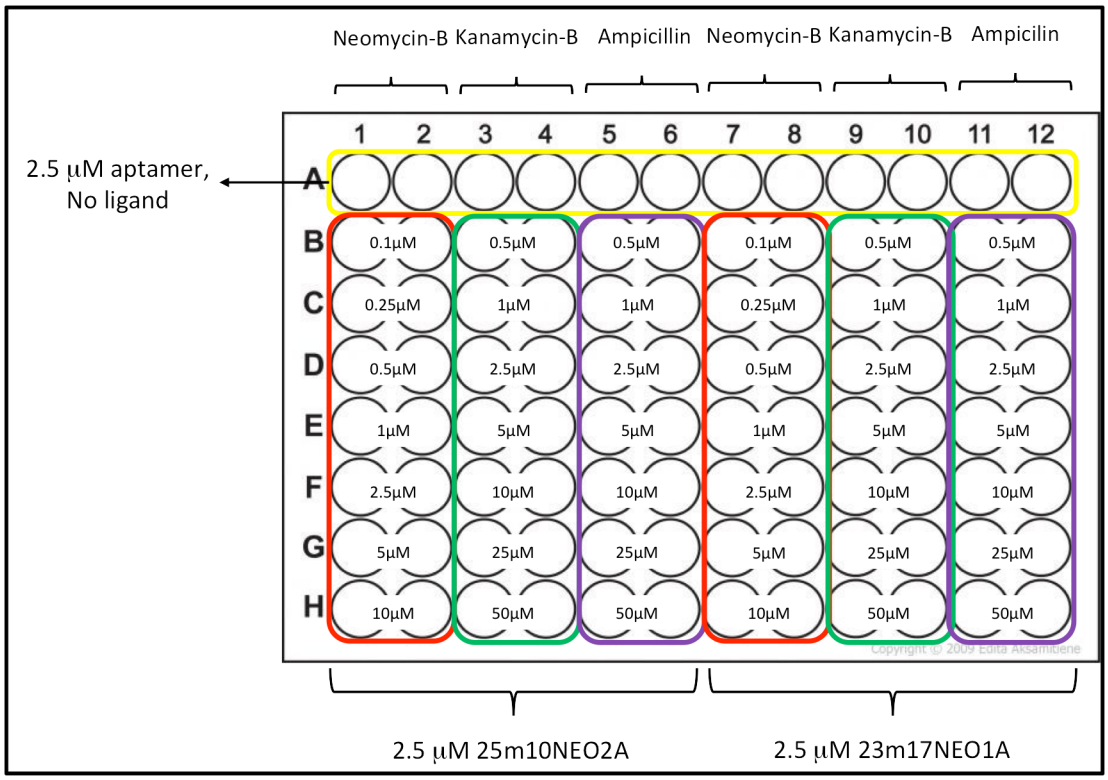

Figure 2.4 96-Well plate design for aptamer and increasing ligand concentrations

Fluorescence measurements are done using the SpectraMax Paradigm plate reader in two repeats. The average values of the obtained data are analyzed using R software.

CHAPTER 3

RESULTS AND DISCUSSION

3.1. ITC Results

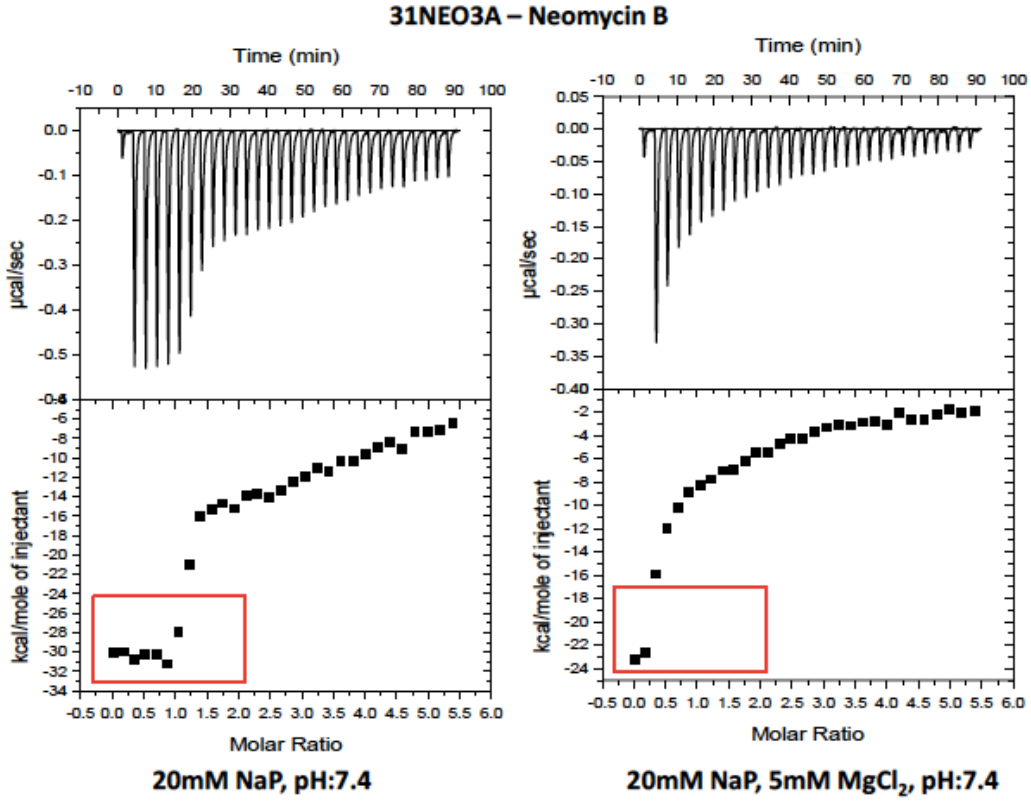

Figure 3.1 Binding curves for 31NEO3A-Neomycin B binding in buffers A and B

As seen in the Figure 3.1, the comparison between 31NEO3A binding to neomycin-B in only NaP (left) buffer and in buffer containing Mg^{2+} ions (right) showed significant difference in binding mode. Addition of 5mM Mg^{2+} into the buffer system has led to a shift from two sets of binding to one set of binding model for this aptamer (indicated in red boxes). This might be due to Mg^{2+} ions chelating around nucleic acids and

blocking the second binding site or competitive binding of Mg^{2+} to the same site as neomycin-B.

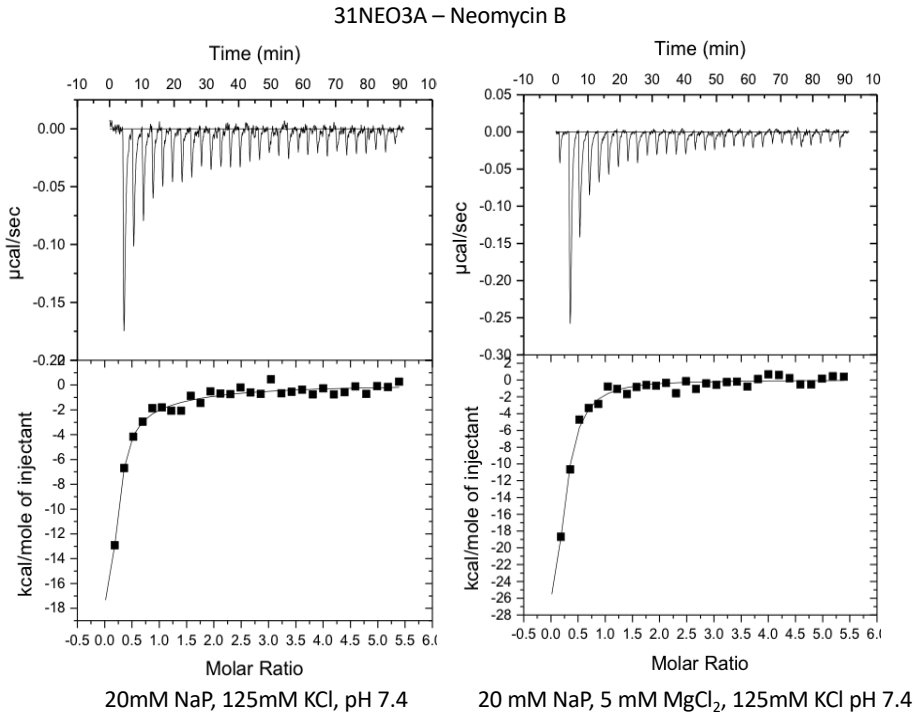

Figure 3.2 Binding curves for 31NEO3A-Neomycin B binding in buffers C and D

Figure 3.2 shows the comparison of 31NEO3A-Neomycin-B binding in Na^+ and K^+ buffer (left), and in Na^+, K^+ and Mg^{2+} containing buffer (right). The binding modes in these buffers are not significantly different, due to high concentrations of metal ions in both environments.

All the aptamers reacted differently to the change in surrounding ion concentrations.

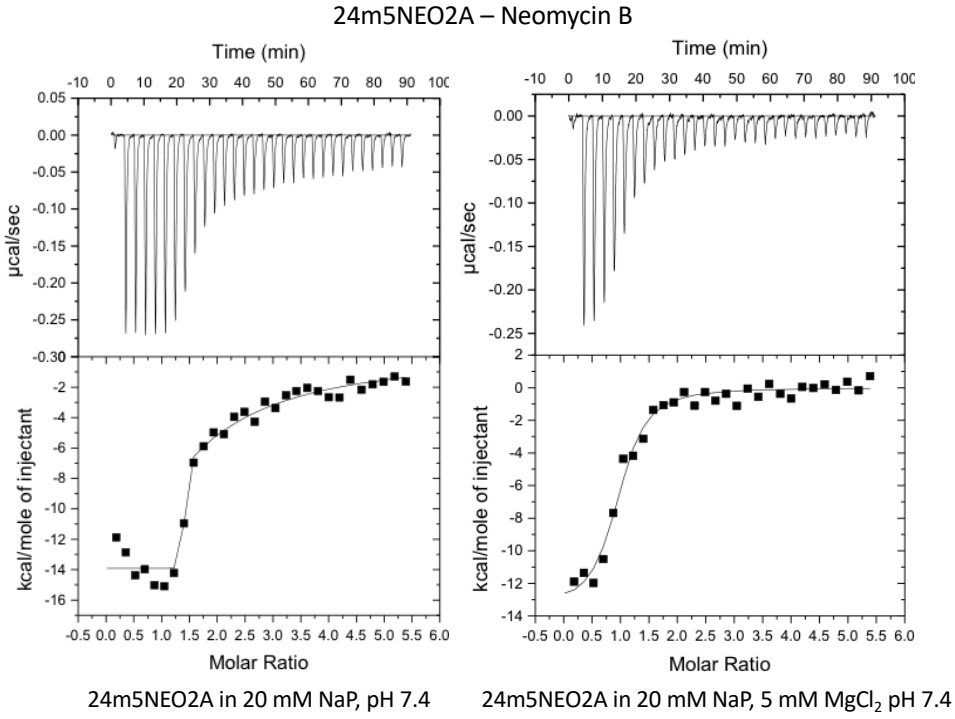

Figure 3.3 Binding curves for 24m5NEO2A-Neomycin B binding in buffers A and B

24m5NEO2A binds to neomycin-B in two sets of binding sites model and with a high affinity in 20mM NaP buffer. Mg^{2+} addition to the buffer leads to a decrease in affinity and a faster saturation rate.

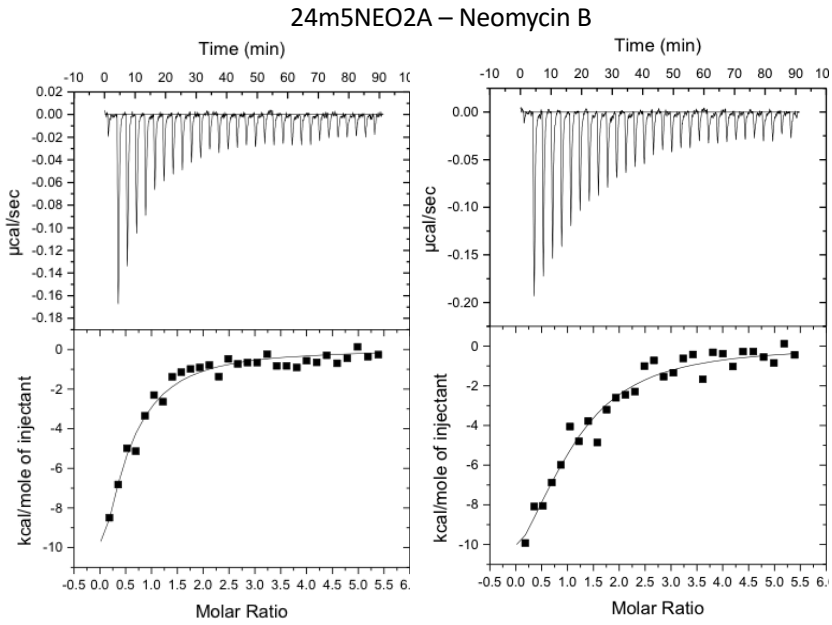

24m5NEO2A in 20 mM NaP, 125 mM KCl pH 7.4 24m5NEO2A in 20 mM NaP, 5 mM $MgCl_2$, 125 mM KCl pH 7.4

Figure 3.4 Binding curves for 24m5NEO2A-Neomycin B binding in buffers C and D

In high monovalent ion concentration, the binding mode of 24m5NEO5A to neomycin-B changed to one binding site mode. The difference in the binding curves suggests that in high K^+ and Mg^{2+} buffer, the saturation rate of the aptamer increased and as a result the affinity decreased.

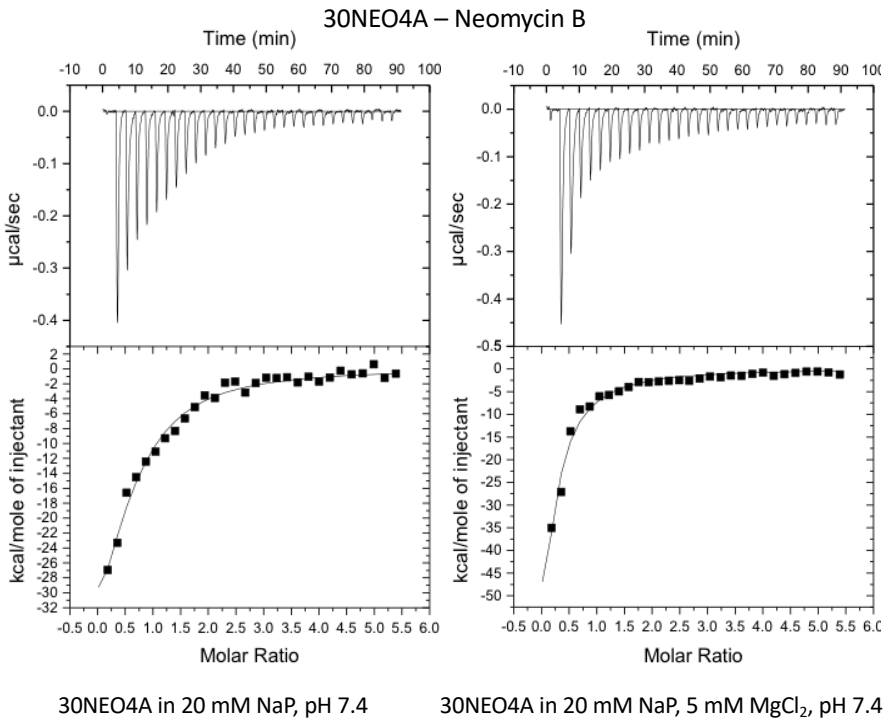

Figure 3.5 Binding curves for 30NEO4A-Neomycin B binding in buffers A and B

30NEO4A-neomycin-B binding mode changed from two binding sites to one binding site mode upon addition of Mg^{2+}. Fast saturation seen in the graph implies that Mg^{2+} addition may block one of the binding sites. In comparison, no significant change in ΔH was observed.

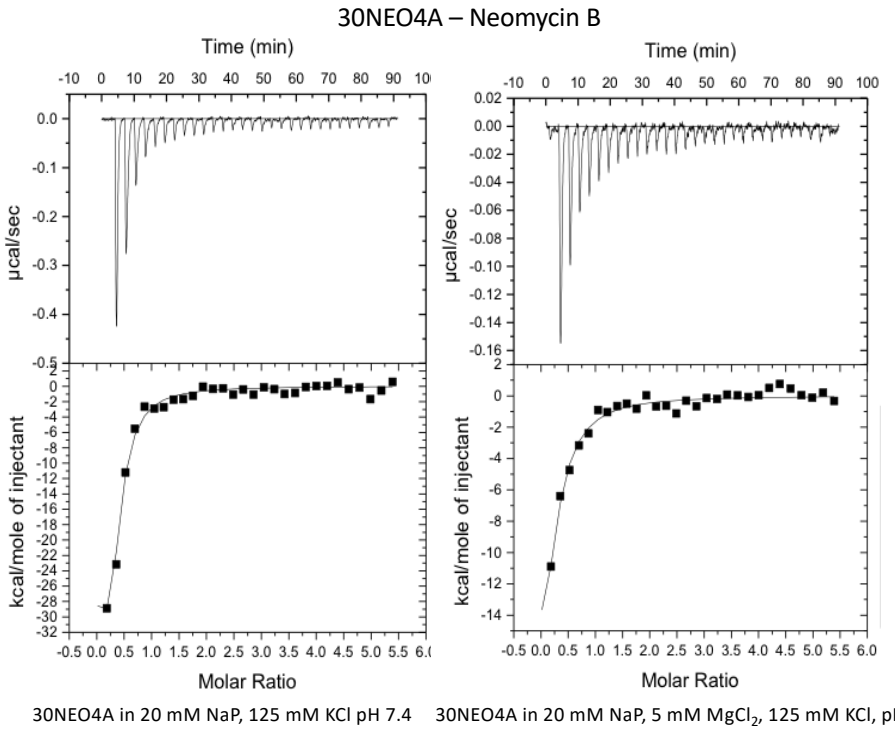

Figure 3.6 Binding curves for 30NEO4A-Neomycin B binding in buffers C and D

30NEO4A-neomycin B binding in high monovalent ion concentration was one binding sites mode and showed a very fast saturation rate. Between the binding graphs from high K^+ buffer and Mg^{2+} buffer (Figure 3.5), no significant change was observed. But upon addition of Mg^{2+} into K^+ buffer, ΔH decreased drastically due to Mg^{2+} binding. Heat release is caused by conformational change and ligand binding. Mg^{2+} compensates for the conformational change by stabilizing the nucleic acid chain. As a result, ligand binding becomes less ΔH dependent.

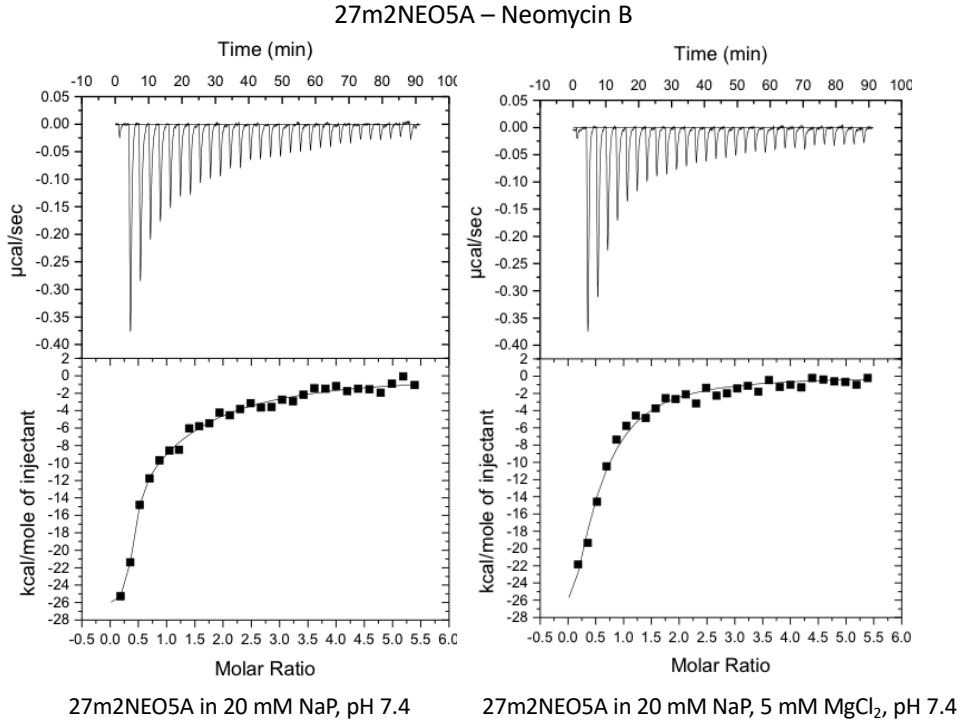

Figure 3.7 Binding curves for 27m2NEO5A-Neomycin B binding in buffers A and B

Binding mode of 27m2NEO5A-neomycin B interaction changed from two binding sites to one binding site models upon Mg^{2+} addition. But, no change in ΔH was observed.

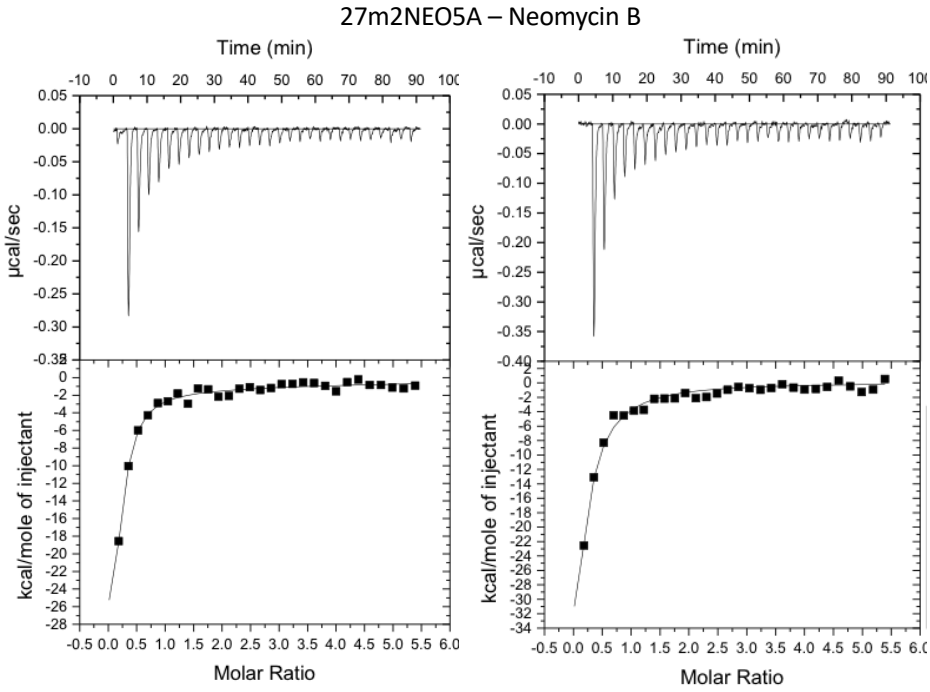

Figure 3.8 Binding curves for 27m2NEO5A-Neomycin B binding in buffers C and D

No significant change was observed for 27m2NEO5A-neomycin-B binding in buffers C and D. Both graphs show one binding site modes and a fast saturation rate.

Table 3.1 K_d values of aptamer-ligand binding in each buffer system

	NaP	**NaP+KCl**	**NaP+$MgCl_2$**	**NaP+KCl+$MgCl_2$**
31NEO3A	Kd_1= 1.25 ± 0.55 µM Kd_2= 0.84 ± 0.58 nM	0.91 ± 0.19 µM	3.31 ± 0.07 µM	0.67 ± 0.29 µM
24m5NEO2A	N/A	1.28 ± 0.43 µM	1.27 ± 0.46 µM	1.58 ± 0.45 µM
30NEO4A	Kd_1= 2.18 ± 1.48 nM Kd_2= 0.69 ± 0.26 µM	0.14 ± 0.03 µM	0.66 ± 0.05 µM	0.48 ± 0.30 µM
27m2NEO5A	Kd_1= 5.12 ± 2.84 nM Kd_2= 2.19 ± 2.03 µM	0.63 ± 0.14 µM	1.24 ± 0.23 µM	1.20 ± 0.27 µM

Table 3.2 ΔS values of aptamer-ligand binding in each buffer system

	NaP	**NaP+KCl**	**NaP+$MgCl_2$**	**NaP+KCl+$MgCl_2$**
31NEO3A	ΔS_1= -13.0 cal/K ΔS_2= -41.6 cal/K	ΔS= -206.92 cal/K	ΔS= -207.46 cal/K	ΔS= -123.2 cal/K
24m5NEO2A	N/A	ΔS= -35.72 cal/K	ΔS= -24.8 cal/K	ΔS= -28.1 cal/K
30NEO4A	ΔS_1= -52.9 cal/K ΔS_2= -49.5 cal/K	ΔS= -86.33 cal/K	ΔS= -95.69 cal/K	ΔS= -97.65 cal/K
27m2NEO5A	ΔS_1= -94.58 cal/K ΔS_2= -37.53 cal/K	ΔS= -235.11 cal/K	ΔS= -144.64 cal/K	ΔS= -158.60 cal/K

Table 3.3 ΔG values of aptamer-ligand binding in each buffer system

	NaP	**NaP+KCl**	**NaP+$MgCl_2$**	**NaP+KCl+$MgCl_2$**
31NEO3A	ΔG_1= 3.8 kcal ΔG_2= 12.26 kcal	ΔG= 59.44 kcal	ΔG= 60.53 kcal	ΔG= 36.44 kcal
24m5NEO2A	N/A	ΔG= 10.54 kcal	ΔG= 7.30 kcal	ΔG= 25.95 kcal
30NEO4A	ΔG_1= 15.61 kcal ΔG_2= 14.62 kcal	ΔG= 24.74 kcal	ΔG= 27.88 kcal	ΔG= 28.89 kcal
27m2NEO5A	N/A	ΔG= 66.30 kcal	ΔG= 43.26 kcal	ΔG= 159.01 kcal

Binding assays with ITC for these aptamers to neomycin B in each buffer were done in two repeats. The results are given as the average K_d values in the Table 3.1. Increasing ion concentrations has led to significant decrease in binding affinities.

Calculated average entropy (ΔS) and Gibbs free energy (ΔG) values are given in tables 3.2 and 3.3, respectively.

3.1.1. Fluorescence Spectroscopy Results

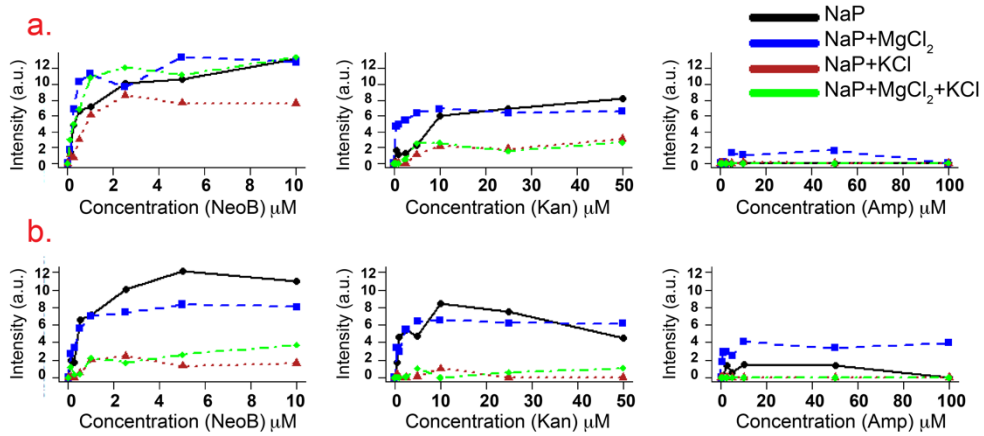

Figure 3.9 Fluorescence measurements obtained from (a) 23m17NEO1A and (b) 25m10NEO2A

The average values of the fluorescence signals from both repeated assays are given as a graph, shown in the Figure 3.9. Both aptamers showed limited binding to kanamycin-B and no binding to ampicillin, so their specificity to neomycin-B was confirmed. Also, for both aptamers, ion dependency was observed, although they differ in response to varying ions.

Kanamycin-B is the same type of antibiotic as neomycin-B and it is known that aminoglycoside aptamers in general may exhibit binding to other aminoglycosides more or less specifically. Fluorescence signals from the aptamers indicate binding to kanamycin-B, as expected, but the signals are decreased compared to neomycin-B binding. 25m10NEO1A in high ionic strength showed binding to Neomycin-B but not to Kanamycin-B.

Both aptamers showed no binding to ampicillin in any buffer system. In the presence of ampicillin, the increased fluorescence signal of 25m10NEO2A is due to diffuse binding of Mg^{2+} ions.

Neomycin-B binding of 23m17NEO1A tended to decrease in high K^+ concentration, but no significant difference was observed as shown in Figure 3.9 (a). 25m10NEO1A displayed best binding to neomycin-B in low metal ion concentration, but in contrast to 23m10NEO1A, significant decrease was observed upon addition of K^+ and Mg^{2+}. These results indicate that both of these aptamers are suitable for neomycin-B detection in solution under low ionic strength and fluorescence measurement can be implemented as the detection system.

Aptamers are affected by the surrounding ions differently. This might be due to their folding patterns in secondary and tertiary structures. Another criterion could be the selection of the site where fluorescent modification is applied. This may also change the aptamer responses to the ligands how they get affected by monovalent and divalent ions that surround residues differently.

CHAPTER 4

CONCLUSION

Aptamers are functional oligonucleotides that can be used in diverse applications. As a result of being nucleic acids in nature, they are expected to be affected by the metal ions in their surrounding environment. The aim of this study was to investigate the behavior of aminoglycoside RNA aptamers under different sets of ionic conditions.

Binding affinity and specificity of aptamers are the two main characteristics that determine the suitability of the aptamers to detect a certain ligand. In this study, we utilized Isothermal Titration Calorimetry (ITC) and Fluorescence Spectroscopy methods to determine such characteristics of selected RNA aptamers.

We observed a significant decrease in affinity upon addition of divalent cations (Mg^{2+}) or high concentrations of monovalent cations (K^{+}) to the buffer system. ITC results showed that, even in low concentrations, addition of Mg^{2+} causes a decline in binding affinity from nM to μM range. Fluorescence measurements also confirmed the ion dependency of aminoglycoside aptamers. They performed the best in low ionic conditions.

As a general statement, we can conclude that even though each aptamer reacted differently to the change ions in their surroundings, their binding affinities drop drastically when exposed to a buffer with high ionic strength. Similarly, their specificities are altered due to the potential conformational change caused by the surrounding ions. In the light of our results, it has become clear that understanding how the aptamers are affected by certain metal ions in solution is critical to get the best performance out of the aptamers. To sum up, the impact of the buffer components should be considered when selecting an aptamer and during the final application.

REFERENCES

Auffinger, P., Grover, N., & Westhof, E. (2011). Metal ion binding to RNA. *Met Ions Life Sci*, *9*, 1–35. Retrieved from http://www.ncbi.nlm.nih.gov/pubmed/22010267

Avery, O. T., Macleod, C. M., & Mc Carty, M. (1994). Studies on the chemical nature of the substance inducing transformation of pneumococcal types: Induction or transformatioby A Desoxyribonucleic acid fraction isolated from pneumococcus type III. *Journal of Experimental Medicine*, *179*(2), 378–384. https://doi.org/10.1084/jem.179.2.379

Azlan, A., Obeidat, S. M., Yunus, M. A., & Azzam, G. (2019). Systematic identification and characterization of Aedes aegypti long noncoding RNAs (lncRNAs). *Scientific Reports*, *9*(1). https://doi.org/10.1038/s41598-019-47506-9

Barnwal, R. P., Yang, F., & Varani, G. (2017). Applications of NMR to structure determination of RNAs large and small. *Archives of Biochemistry and Biophysics*. https://doi.org/10.1016/j.abb.2017.06.003

Basu, S., Rambo, R. P., Strauss-Soukup, J., Cate, J. H., Ferré-D'Amaré, A. R., Strobel, S. A., & Doudna, J. A. (1998). A specific monovalent metal ion integral to the AA platform of the RNA tetraloop receptor. *Nature Structural Biology*, *5*(11), 986–992. https://doi.org/10.1038/2960

Batey, R. T., Rambo, R. P., Lucast, L., Rha, B., & Doudna, J. A. (2000). Crystal structure of the ribonucleoprotein core of the signal recognition particle. *Science*, *287*(5456), 1232–1239. https://doi.org/10.1126/science.287.5456.1232

Breuers, S., Bryant, L. L., Legen, T., & Mayer, G. (2019). Robotic assisted generation of 2′-deoxy-2′-fluoro-modifed RNA aptamers – High performance enabling strategies in aptamer selection. *Methods*, *161*, 3–9. https://doi.org/10.1016/j.ymeth.2019.05.022

Butcher, S. E., Dieckmann, T., & Feigon, J. (1997). Solution structure of the conserved 16 S-like ribosomal RNA UGAA tetraloop. *Journal of Molecular Biology*. https://doi.org/10.1006/jmbi.1997.0964

Cassini, A., Högberg, L. D., Plachouras, D., Quattrocchi, A., Hoxha, A., Simonsen, G. S., … Hopkins, S. (2018). Attributable deaths and disability-adjusted life-years caused by infections with antibiotic-resistant bacteria in the EU and the European Economic Area in 2015: a population-level modelling analysis. *The Lancet Infectious Diseases*. https://doi.org/10.1016/S1473-3099(18)30605-4

Cate, J. H., & Doudna, J. A. (1996). Metal-binding sites in the major groove of a large

ribozyme domain. *Structure*, *4*(10), 1221–1229. https://doi.org/10.1016/S0969-2126(96)00129-3

Chang, A. L., McKeague, M., Liang, J. C., & Smolke, C. D. (2014). Kinetic and equilibrium binding characterization of aptamers to small molecules using a label-free, sensitive, and scalable platform. *Analytical Chemistry*. https://doi.org/10.1021/ac5001527

Chial, H. (2008). DNA sequencing technologies key to the Human Genome Project. *Nature Education*, *1*(1), 219. Retrieved from http://www.nature.com/scitable/topicpage/DNA-Sequencing-Technologies-Key-to-the-Human-828?auTags=

Chin, K., Sharp, K. A., Honig, B., & Pyle, A. M. (1999). Calculating the electrostatic properties of RNA provides new insights into molecular interactions and function. *Nature Structural Biology*, *6*(11), 1055–1061. https://doi.org/10.1038/14940

Chittapragada, M., Roberts, S., & Ham, Y. W. (2009). Aminoglycosides: Molecular insights on the recognition of RNA and aminoglycoside mimics. *Perspectives in Medicinal Chemistry*, Vol. 2009, pp. 21–37. https://doi.org/10.4137/pmc.s2381

Clancy, S. (2008). RNA Functions. *Nature Education*, *1*(2008), 1–5.

Correll, C. C., Freeborn, B., Moore, P. B., & Steitz, T. A. (1997). Metals, motifs, and recognition in the crystal structure of a 5S rRNA domain. *Cell*, *91*(5), 705–712. https://doi.org/10.1016/S0092-8674(00)80457-2

Dahm, R. (2008). Discovering DNA: Friedrich Miescher and the early years of nucleic acid research. *Human Genetics*, Vol. 122, pp. 565–581. https://doi.org/10.1007/s00439-007-0433-0

Dahm, R. (2010). From discovering to understanding. *EMBO Reports*. https://doi.org/10.1038/embor.2010.14

Draper, D. E. (2004). A guide to ions and RNA structure. *Rna*, Vol. 10, pp. 335–343. https://doi.org/10.1261/rna.5205404

Duff, M. R., Grubbs, J., & Howell, E. E. (2011). Isothermal titration calorimetry for measuring macromolecule-ligand affinity. *Journal of Visualized Experiments*. https://doi.org/10.3791/2796

Dunn, M. R., Jimenez, R. M., & Chaput, J. C. (2017). Analysis of aptamer discovery and technology. *Nature Reviews Chemistry*. https://doi.org/10.1038/s41570-017-0076

E. Wang, R., Wu, H., Niu, Y., & Cai, J. (2011). Improving the Stability of Aptamers by Chemical Modification. *Current Medicinal Chemistry*, *18*(27), 4126–4138. https://doi.org/10.2174/092986711797189565

Edwards, B. A. L., & Batey, R. T. (2010). Riboswitches : A Common RNA Regulatory Element. *Nature Education*. https://doi.org/http://www.nature.com/scitable/topicpage/riboswitches-a-common-rna-regulatory-element-14262702

Ellington, A. D., & Szostak, J. W. (1990). In vitro selection of RNA molecules that bind specific ligands. *Nature*, *346*(6287), 818–822. https://doi.org/10.1038/346818a0

Ferré-D'Amaré, A. R., & Doudna, J. A. (2000). Methods to Crystallize RNA. In *Current Protocols in Nucleic Acid Chemistry*. https://doi.org/10.1002/0471142700.nc0706s00

Fourmy, D., Recht, M. I., Blanchard, S. C., & Puglisi, J. D. (1996). Structure of the A site of Escherichia coli 16S ribosomal RNA complexed with an aminoglycoside antibiotic. *Science*, *274*(5291), 1367–1371. https://doi.org/10.1126/science.274.5291.1367

Furusawa, C., Horinouchi, T., & Maeda, T. (2018). Toward prediction and control of antibiotic-resistance evolution. *Current Opinion in Biotechnology*. https://doi.org/10.1016/j.copbio.2018.01.026

Germovsek, E., Barker, C. I., & Sharland, M. (2017). What do i need to know about aminoglycoside antibiotics? *Archives of Disease in Childhood: Education and Practice Edition*, *102*(2), 89–93. https://doi.org/10.1136/archdischild-2015-309069

Goff, L. A., & Rinn, J. L. (2015). Linking RNA biology to lncRNAs. *Genome Research*. https://doi.org/10.1101/gr.191122.115

Hasegawa, H., Savory, N., Abe, K., & Ikebukuro, K. (2016). Methods for improving aptamer binding affinity. *Molecules*, Vol. 21. https://doi.org/10.3390/molecules21040421

HERSHEY, A. D., & CHASE, M. (1952). Independent functions of viral protein and nucleic acid in growth of bacteriophage. *The Journal of General Physiology*, *36*(1), 39–56. https://doi.org/10.1085/jgp.36.1.39

Ilgu, M., Fazlioglu, R., Ozturk, M., Ozsurekci, Y., & Nilsen-Hamilton, M. (2019). Aptamers for Diagnostics with Applications for Infectious Diseases. In M. Ince & O. K. Ince (Eds.), *Recent Advances in Analytical Chemistry*. https://doi.org/10.5772/intechopen.84867

Ilgu, M., Fulton, D. B., Yennamalli, R. M., Lamm, M. H., Sen, T. Z., & Nilsen-Hamilton, M. (2014). An adaptable pentaloop defines a robust neomycin-B RNA aptamer with conditional ligand-bound structures. *RNA*, *20*(6), 815–824. https://doi.org/10.1261/rna.041145.113

Jiang, L, Majumdar, A., Hu, W., Jaishree, T. J., Xu, W., & Patel, D. J. (1999).

Saccharide-RNA recognition in a complex formed between neomycin B and an RNA aptamer. *Structure*, *7*(7), 817–827. Retrieved from http://www.ncbi.nlm.nih.gov/pubmed/10425683

Jiang, Licong, Suri, A. K., Fiala, R., & Patel, D. J. (1997). Saccharide-RNA recognition in an aminoglycoside antibiotic-RNA aptamer complex. *Chemistry and Biology*. https://doi.org/10.1016/S1074-5521(97)90235-0

Johnson-Buck, A. E., McDowell, S. E., & Walter, N. G. (2011). Metal ions: supporting actors in the playbook of small ribozymes. *Metal Ions in Life Sciences*. https://doi.org/10.1515/9783110436648-011

Kazakov, S. A., & Hecht, S. M. (2016). *Nucleic Acid – Metal Ion Interactions Nucleic Acid – Metal Ion Interactions*. https://doi.org/10.1002/0470862106.ia166

Keefe, A. D., & Cload, S. T. (2008). SELEX with modified nucleotides. *Current Opinion in Chemical Biology*, Vol. 12, pp. 448–456. https://doi.org/10.1016/j.cbpa.2008.06.028

Klug, S. J., & Famulok, M. (1994). All you wanted to know about SELEX. *Molecular Biology Reports*, *20*(2), 97–107. https://doi.org/10.1007/BF00996358

Krause, K. M., Serio, A. W., Kane, T. R., & Connolly, L. E. (2016). Aminoglycosides: An overview. *Cold Spring Harbor Perspectives in Medicine*, *6*(6). https://doi.org/10.1101/cshperspect.a027029

Kulik, M., Goral, A. M., Jasiński, M., Dominiak, P. M., & Trylska, J. (2015). Electrostatic interactions in aminoglycoside-RNA complexes. *Biophysical Journal*, *108*(3), 655–665. https://doi.org/10.1016/j.bpj.2014.12.020

Kwon, M., Chun, S. M., Jeong, S., & Yu, J. (2001). In vitro selection of RNA against kanamycin B. *Molecules and Cells*, *11*(3), 303–311.

Lato, S. M., Boles, A. R., & Ellington, A. D. (1995). In vitro selection of RNA lectins: using combinatorial chemistry to interpret ribozyme evolution. *Chemistry and Biology*, *2*(5), 291–303. https://doi.org/10.1016/1074-5521(95)90048-9

Lipfert, J., Doniach, S., Das, R., & Herschlag, D. (2014). Understanding Nucleic Acid–Ion Interactions. *Annual Review of Biochemistry*. https://doi.org/10.1146/annurev-biochem-060409-092720

Lorenz, C., & Schroeder, R. (2006). Aptamers to Antibiotics. In *The Aptamer Handbook: Functional Oligonucleotides and Their Applications*. https://doi.org/10.1002/3527608192.ch5

McCluskey, K., Boudreault, J., St-Pierre, P., Perez-Gonzalez, C., Chauvier, A., Rizzi, A., … Penedo, J. C. (2019). Unprecedented tunability of riboswitch structure and regulatory function by sub-millimolar variations in physiological Mg2+. *Nucleic Acids Research*, *47*(12), 6478–6487. https://doi.org/10.1093/nar/gkz316

Mehlhorn, A., Rahimi, P., & Joseph, Y. (2018). Aptamer-Based Biosensors for Antibiotic Detection: A Review. *Biosensors*, *8*(2), 54. https://doi.org/10.3390/bios8020054

Mikkelsen, N. E., Johansson, K., Virtanen, A., & Kirsebom, L. A. (2001). Aminoglycoside binding displaces a divalent metal ion in a tRNA-neomycin B complex. *Nature Structural Biology*, *8*(6), 510–514. https://doi.org/10.1038/88569

Nam, J. W., & Bartel, D. P. (2012). Long noncoding RNAs in C. elegans. *Genome Research*, *22*(12), 2529–2540. https://doi.org/10.1101/gr.140475.112

Näslund, P. H., & Hultin, T. (1971). Structural and functional defects in mammalian ribosomes after potassium deficiency. *BBA Section Nucleic Acids And Protein Synthesis*. https://doi.org/10.1016/0005-2787(71)90117-1

Ni, S., Yao, H., Wang, L., Lu, J., Jiang, F., Lu, A., & Zhang, G. (2017). Chemical modifications of nucleic acid aptamers for therapeutic purposes. *International Journal of Molecular Sciences*, Vol. 18. https://doi.org/10.3390/ijms18081683

Noeske, J., Schwalbe, H., & Wöhnert, J. (2007). Metal-ion binding and metal-ion induced folding of the adenine-sensing riboswitch aptamer domain. *Nucleic Acids Research*, *35*(15), 5262–5273. https://doi.org/10.1093/nar/gkm565

Parisien, M., & Major, F. (2008). The MC-Fold and MC-Sym pipeline infers RNA structure from sequence data. *Nature*, *452*(7183), 51–55. https://doi.org/10.1038/nature06684

Pyle, A. M. (2002). Metal ions in the structure and function of RNA. *Journal of Biological Inorganic Chemistry*, Vol. 7, pp. 679–690. https://doi.org/10.1007/s00775-002-0387-6

Ramakrishnan, V. (2002). Ribosome structure and the mechanism of translation. *Cell*. https://doi.org/10.1016/S0092-8674(02)00619-0

Robertson, D. L., & Joyce, G. F. (1990). Selection in vitro of an RNA enzyme that specifically cleaves single-stranded DNA. *Nature*, *344*(6265), 467–468. Retrieved from http://www.ncbi.nlm.nih.gov/entrez/query.fcgi?cmd=Retrieve&db=PubMed&dopt=Citation&list_uids=1690861

Rosenbloom, K. R., Dreszer, T. R., Long, J. C., Malladi, V. S., Sloan, C. A., Raney, B. J., … Kent, W. J. (2012). ENCODE whole-genome data in the UCSC Genome Browser: Update 2012. *Nucleic Acids Research*, *40*(D1). https://doi.org/10.1093/nar/gkr1012

Rozov, A., Khusainov, I., El Omari, K., Duman, R., Mykhaylyk, V., Yusupov, M., … Yusupova, G. (2019). Importance of potassium ions for ribosome structure and function revealed by long-wavelength X-ray diffraction. *Nature*

Communications. https://doi.org/10.1038/s41467-019-10409-4

Serganov, A., & Patel, D. J. (2012). Metabolite Recognition Principles and Molecular Mechanisms Underlying Riboswitch Function. *Annual Review of Biophysics*. https://doi.org/10.1146/annurev-biophys-101211-113224

Song, K. M., Lee, S., & Ban, C. (2012). Aptamers and their biological applications. *Sensors*. https://doi.org/10.3390/s120100612

Stampfl, S., Lempradl, A., Koehler, G., & Schroeder, R. (2007). Monovalent ion dependence of neomycin B binding to an RNA aptamer characterized by spectroscopic methods. *Chembiochem*, *8*(10), 1137–1145. https://doi.org/10.1002/cbic.200700030

Tombelli, S., Minunni, M., & Mascini, M. (2005). Analytical applications of aptamers. *Biosensors and Bioelectronics*. https://doi.org/10.1016/j.bios.2004.11.006

Tuerk, C., & Gold, L. (1990). Systematic evolution of ligands by exponential enrichment: RNA ligands to bacteriophage T4 DNA polymerase. *Science*, *249*(4968), 505–510. https://doi.org/10.1126/science.2200121

Vakulenko, S. B., & Mobashery, S. (2003). Versatility of aminoglycosides and prospects for their future. *Clinical Microbiology Reviews*. https://doi.org/10.1128/CMR.16.3.430-450.2003

Wallis, M. G., von Ahsen, U., Schroeder, R., & Famulok, M. (1995). A novel RNA motif for neomycin recognition. *Chemistry and Biology*, *2*(8), 543–552. https://doi.org/10.1016/1074-5521(95)90188-4

Wang, Y., & Rando, R. R. (1995). Specific binding of aminoglycoside antibiotics to RNA. *Chemistry and Biology*, *2*(5), 281–290. https://doi.org/10.1016/1074-5521(95)90047-0

Watson, J. D., & Crick, F. H. C. (1969). Molecular structure of Nucleic acids: A structure for Deoxyribose Nucleic acid (Reprinted from Nature, April 25, 1953). *Nature*, *224*(5218), 470–471. https://doi.org/10.1038/224470a0

Watson, P. Y., & Fedor, M. J. (2011). The glmS riboswitch integrates signals from activating and inhibitory metabolites in vivo. *Nature Structural and Molecular Biology*. https://doi.org/10.1038/nsmb.1989

Weigand, J. E., Schmidtke, S. R., Will, T. J., Duchardt-Ferner, E., Hammann, C., Wöhnert, J., & Suess, B. (2011). Mechanistic insights into an engineered riboswitch: A switching element which confers riboswitch activity. *Nucleic Acids Research*. https://doi.org/10.1093/nar/gkq946

Wengerter, B. C., Katakowski, J. A., Rosenberg, J. M., Park, C. G., Almo, S. C., Palliser, D., & Levy, M. (2014). Aptamer-targeted antigen delivery. *Molecular*

Therapy. https://doi.org/10.1038/mt.2014.51

Westhof, E. (2015). Twenty years of RNA crystallography. *Rna*, Vol. 21, pp. 486–487. https://doi.org/10.1261/rna.049726.115

Woodson, S. A. (2005). Metal ions and RNA folding: A highly charged topic with a dynamic future. *Current Opinion in Chemical Biology*, Vol. 9, pp. 104–109. https://doi.org/10.1016/j.cbpa.2005.02.004

Xi, K., Wang, F. H., Xiong, G., Zhang, Z. L., & Tan, Z. J. (2018). Competitive Binding of Mg2+ and Na+ Ions to Nucleic Acids: From Helices to Tertiary Structures. *Biophysical Journal*. https://doi.org/10.1016/j.bpj.2018.03.001

Zhang, J., Sui, S., Wu, H., Zhang, J., Zhang, X., Xu, S., & Pang, D. (2019). The transcriptional landscape of lncRNAs reveals the oncogenic function of LINC00511 in ER-negative breast cancer. *Cell Death & Disease*, *10*(8). https://doi.org/10.1038/s41419-019-1835-3

Zhang, Y., Lai, B. S., & Juhas, M. (2019). Recent advances in aptamer discovery and applications. *Molecules*. https://doi.org/10.3390/molecules24050941

Zhuo, Z., Yu, Y., Wang, M., Li, J., Zhang, Z., Liu, J., … Zhang, B. (2017). Recent advances in SELEX technology and aptamer applications in biomedicine. *International Journal of Molecular Sciences*, Vol. 18. https://doi.org/10.3390/ijms18102142

APPENDICES

A. ITC Parameters

- Number of injections: 30
- Temperature: 25 ºC
- Reference power: 18 µcal/sec
- Initial delay: 60 sec
- Syringe concentration: 0.060 mM
- Cell concentration: 0.0025 mM
- Stirring speed: 300 rpm
- Injection volume: 10 µL (first injection 1µL)
- Duration: 20 sec (first injection 2 sec)
- Spacing: 180 sec
- Filler period: 2 sec